**-1BRIEF REPORT**

# Endogenous ZAP is associated with altered Zika virus infection phenotype

**Nguyen Phuong Khanh Le[1], Prince Pal Singh[1,2], Ahmad Jawad Sabir[3], Ivan Trus[4], Uladzimir Karniychuk[1,*]**

[1]Department of Veterinary Biosciences, College of Veterinary Medicine, The Ohio State University, Columbus, OH, USA

[2]School of Public Health, University of Saskatchewan, Saskatoon, Canada

[3]Department of Microbiology and Immunology, University of Illinois, College of Medicine, Chicago, IL, USA

[4]Dioscuri Centre for RNA-Protein Interactions in Human Health and Disease, International Institute of Molecular and Cell Biology, Warsaw, Poland

*** Correspondence:** Uladzimir Karniychuk

Department of Veterinary Biosciences, College of Veterinary Medicine, The Ohio State University, Columbus, OH, USA

karniychuk.1@osu.edu

**Abstract**

The zinc finger antiviral protein 1 (ZAP) has broad antiviral activity. ZAP is an interferon (IFN)-stimulated gene, which itself may enhance type I IFN antiviral response. In a previous study, Zika virus was identified as ZAP-resistant and not sensitive to ZAP antiviral activity. Here, we found that ZAP was associated with the inhibition of Zika virus in Vero cells, in the absence of a robust type I IFN system because Vero cells are deficient for IFN-alpha and -beta. Also, quantitative RNA-seq data indicated that endogenous ZAP is associated with altered global gene expression both in the steady state and during Zika virus infection. Further studies are warranted to elucidate this IFN-alpha and -beta independent anti-Zika virus activity and involvement of ZAP.

**Keywords**: **Flavivirus, Zika virus, Zinc finger antiviral protein, ZAP, interferon, RNA-seq**

46 **INTRODUCTION**

47 The zinc finger CCCH-type antiviral protein 1 (ZAP) is a cellular protein with broad antiviral
48 activity (1, 2, 3, 4, 5). ZAP targets CpG-rich regions of RNA and ZAP binding to viral RNA
49 mediates its degradation and translational inhibition (3, 6). While ZAP lacks intrinsic RNase
50 activity, it recruits the 5′ and 3′ RNA degradation machinery (7, 8). Using a murine leukemia
51 reporter virus, DDX17 and DHX30 cellular RNA helicases were identified as ZAP co-factors (9,
52 10). The E3 ubiquitin ligase TRIM25 enhances ZAP activity against alphaviruses (11, 12). ZAP
53 also interacts with the cytoplasmic protein KHNYN to inhibit CpG-enriched human
54 immunodeficiency virus 1 (HIV-1) (13). Recently, Riplet, a protein known for activating the
55 retinoic acid-inducible gene I, was identified as a ZAP co-factor (14). Initially characterized to
56 inhibit murine leukemia virus (15), ZAP has shown efficacy against many viruses, including
57 alphaviruses, filoviruses, influenza virus, porcine reproductive and respiratory syndrome virus,
58 hepatitis B virus, human cytomegalovirus, human T-cell lymphotropic virus type 1, and HIV-1
59 (1, 6, 16, 17, 18, 19, 20, 21, 22, 23, 24). However, ZAP's antiviral efficiency is limited against
60 certain RNA viruses, including vesicular stomatitis virus, poliovirus, enterovirus A71, herpes
61 simplex virus type 1, and some flaviviruses (8, 16, 25). Emerging flaviviruses constantly threaten
62 public health. A previous study showed the sensitivity of Japanese encephalitis virus (JEV) to
63 overexpressed ectopic and endogenous ZAP (8). In contrast, yellow fever virus (YFV), dengue
64 virus (DENV), and Zika virus were categorized as ZAP-resistant (8, 16). These are interesting
65 findings because all these flaviviruses have underrepresented CpG content (**Fig S1**) which may
66 help to avoid ZAP recognition (3, 6); however, JEV has the least underrepresented CpG content
67 (**Fig S1**) which supports higher sensitivity to ZAP (8). Here, we further extended studies on

68 ZAP-flavivirus interactions and compared Zika virus infection and transcriptional responses in
69 wild-type and ZAP knockout Vero cells.
70
71 **MATERIALS AND METHODS**
72 **Cells**
73 We maintained wild-type Vero E6 cells (ATCC; Vero-ZAP-WT) and ZAP knockout (ZAP-KO)
74 derivatives (Vero-ZAP-KO) in DMEM (Fisher; # 11-965-118) supplemented with 10% heat-
75 inactivated fetal bovine serum (FBS, Fisher; #A5256801), 1x Penicillin-Streptomycin (Fisher;
76 #15140122), and 2.67 mM sodium bicarbonate (Fisher; # 25080094) at +37°C in a 5% $CO_2$
77 humidified incubator. To generate ZAP-KO cell line, we used the guide RNA (gRNA)
78 GTCTCTGGCAGTACTTGCGA which targets the first exon of *Chlorocebus sabaeus* (Gene ID:
79 103226990) ZC3HAV1 gene, which is required for the expression of all ZAP isoforms. We also
80 used a non-targeting control gRNA ACGGAGGCTAAGCGTCGCAA for control cells. These
81 gRNAs were transiently transfected into cells using GenCrispr NLS-Cas9-NLS Nuclease
82 (GenScript). Subsequently, transfected cells were seeded in 96-well plates through limiting
83 dilution to generate isogenic single clones. Following expansion, the clones were genotyped via
84 Sanger sequencing, employing primers (ATCGCTGGGCTGGACTAACG,
85 GCAGAGAAGGGAGTGGCTGAA) to identify indels (location of indels on *Chlorocebus*
86 *sabaeus* genome: -2bp deletion, NW_023666072.1: 4677550-4677551). The knockout subclone
87 verified by genotyping was further confirmed by western blot for ZAP expression (**Fig 1A, Fig**
88 **S2**) as described below. The negative control cells were validated by Sanger sequencing to
89 confirm there were no indels. We confirmed the absence of mycoplasma contamination in cells
90 using the LookOut Mycoplasma PCR Detection Kit (Millipore Sigma).

91 **Viruses**

92 We utilized the Asian lineage Zika virus H/PF/2013 strain [GenBank: KJ776791.2]. Zika virus
93 was rescued using reverse genetics (26). Subsequently, the virus was propagated in Vero cells
94 cultured in DMEM supplemented with 2% FBS and 1% penicillin/streptomycin. Supernatants
95 were harvested, centrifuged (12,000 g, 20 min, +4°C), aliquoted, and frozen (-80°C). Infectious
96 virus titers were quantified using Vero cells via and endpoint dilution assay. The fifty percent
97 tissue culture infective dose ($TCID_{50}$) endpoint titers were calculated as previously described
98 (26, 27, 28, 29). Media from virus-negative Vero cells were processed in the same manner as the
99 virus stocks and used as control. The absence of mycoplasma contamination in the virus stocks
100 was confirmed using the LookOut Mycoplasma PCR Detection Kit (Millipore Sigma;
101 #MP0035).

102

103 **Zika virus infection kinetics**

104 Vero-ZAP-WT and Vero-ZAP-KO cells were seeded in 6-well plates in DMEM supplemented
105 with 10% inactivated fetal bovine serum for 24 h. Four wells for each cell line, representing four
106 biological replicates (cells from different passages and flasks in each of 4 wells), were inoculated
107 with Zika virus at a multiplicity of infection (MOI) of 1. After 2 h at 37ºC, the inoculum was
108 removed, the cells were washed three times, covered with 3 ml of DMEM supplemented with
109 2% FBS, and maintained at 37ºC. At 2, 24, 48, 72, 96, and 120 h post-inoculation, 150 µl of
110 media supernatants were collected, cleared by centrifugation (2,000 g, 10 min), and frozen at -
111 80°C for the end-point dilution $TCID_{50}$ assay (26, 29, 30, 31, 32, 33).

112

113

114 **Western blot**

115 Untreated, mock-infected, or Zika-infected (MOI 1) Vero-ZAP-WT and Vero-ZAP-KO cells
116 were washed, pelletized, and lysed in 100 µL of RIPA buffer (Fisher; # PI89900) supplemented
117 with 1× Halt protease inhibitor cocktail (Fisher; #PI87786) and 1× EDTA (Fisher; #BP2473100).
118 The lysates were then incubated on wet ice for 10 minutes, gently vortexed, and centrifuged
119 (12,000g, 10 min, +4 °C). Supernatants were aliquoted into prechilled low protein-binding
120 (Sarstedt; #72.706.600) and stored at -80°C. After quantifying protein concentration with the
121 Pierce BCA Protein Assay Kit (Fisher; # PI23227), 50 µg of protein extract was diluted in 4×
122 reducing Laemmli SDS sample buffer (Fisher; #AAJ60015AC), heated at 95ºC for 10 min, and
123 resolved on 10% Mini-PROTEAN TGX precast protein gels (Bio-Rad; # 4561035) in 1×
124 Tris/Glycine/SDS running buffer (Bio-Rad; #1610732) at a voltage of 125V for 70 min. Proteins
125 were transferred on methanol-activated 0.45 µm Immun-Blot Low Fluorescence polyvinylidene
126 fluoride (PVDF) membranes using the Trans-Blot Turbo RTA Mini 0.45 µm LF PVDF Transfer
127 Kit (Bio-Rad; #1704274). The PVDF membranes were blocked with 1× VWR Life Science
128 Rapidblock Blocking Solution (VWR; #97064-124) for 1 h at room temperature. Subsequently,
129 the membranes were incubated overnight at +4°C with primary antibody diluted in blocking
130 solution. The membranes were washed four times with TBST (1× Bio-Rad Tris Buffered Saline
131 containing 0.1% Tween-20) and then incubated with secondary antibody, along with hFAB
132 Rhodamine Anti-Actin Primary Antibody (Recombinant human β-actin), diluted in Blocking
133 Solution for 1 h at room temperature, and washed four times with TBST. Fluorescent blots were
134 imaged on the ChemiDoc MP Imaging system using an appropriate detection channel with
135 Image Lab Touch Software (Bio-Rad).

136 We used antibodies (Abs): Rabbit anti-ZAP IgG Abs (1:1,000 dilution; ANTI-ZC3HAV1;
137 #HPA059096-100UL, Sigma-Aldrich), Rabbit anti-Zika virus NS5 IgG Abs (1:1,000 dilution;
138 #GTX133312, GeneTex), hFAB Rhodamine Anti-Actin Primary Abs (1:2,500; #12004164, Bio-
139 Rad), and IRDye 680RD Goat anti-Rabbit IgG secondary Abs (1:10,000; #926-68071; LI-COR).
140

141 **Comparative RNA-seq analysis in wild-type and ZAP-KO cells**

142 Vero-ZAP-WT and Vero-ZAP-KO cells were seeded at $6\times10^5$ cells per well in 6-well plates,
143 with 4 plates per cell line, in DMEM supplemented with 10% FBS for 24 h. Wells in two plates
144 from each cell line were either mock-inoculated with media from virus-negative cells (4-6 well
145 replicates for Vero-ZAP-WT and Vero-ZAP-KO) or inoculated with MOI 1 of Zika virus (6 well
146 replicates for Vero-ZAP-WT and Vero-ZAP-KO). After 2 h at 37ºC, the inoculum was removed,
147 cells were washed, and covered with DMEM supplemented with 2% FBS, then maintained at
148 37ºC. At 24 h and 72 h post-inoculation, media was removed, cells were washed with
149 commercial 1× PBS, homogenized in 1 mL of TRI Reagent Solution (Fisher; # AM9738), and
150 RNA was extracted according to the manufacturer's protocol using the PureLink RNA Mini Kit
151 (Fisher; 12-183-018A). A total of 4-6 replicate samples were obtained for mock-inoculated
152 Vero-ZAP-WT, mock-inoculated Vero-ZAP-KO, Zika-infected Vero-ZAP-WT, and Zika-
153 infected Vero-ZAP-KO cells, at both 24 and 72 h. Zika infection was confirmed by virus-specific
154 RT-qPCR with a previously validated SYBR one-step RT-qPCR assay (26, 28, 34). RNA
155 quantification was performed using the Qubit RNA High Sensitivity kit (Fisher; # Q32855) and
156 Qubit 2.0 Fluorometer (Fisher). RNA quality was assessed using a bioanalyzer (Agilent
157 Technologies 2100) to ensure all samples had RNA Integrity Number (RIN) values above 9.0.
158 DNA contamination was removed using the TURBO DNA-free Kit (Fisher; # AM1907). mRNA

159 with intact poly(A) tails was enriched using the NEBNext Poly(A) mRNA Magnetic Isolation
160 Module (NEB; # E7490L) and utilized for library constructions with the NEBNext Ultra II
161 Directional RNA Library Prep Kit for Illumina along with NEBNext Multiplex Oligos for
162 Illumina (96 Unique Dual Index Primer Pairs; NEB; # E7760L). The libraries were sequenced on
163 the NovaSeq platform as paired-end reads using the S1 v1.5 kit with 300 cycles (Illumina). Raw
164 sequencing data were deposited to NCBI BioProject (PRJNA1101086).
165
166 FASTQ files were trimmed for adaptor sequences and filtered for low-quality reads using
167 *Trimmomatic*. RNA-seq analysis was conducted as previously described (29, 30, 33, 35) with
168 modifications. Briefly, paired-end reads were processed using the *Kallisto* pseudo-alignment
169 method (36) and quantified by mapping to a transcripts database generated from the African
170 Green Monkey (vervet) reference genome assembly (ENSEMBL *Chlorocebus sabaeus* 1.1) (37).
171 The count table for RNA-seq data was assembled using the *tximport::tximport* function in R.
172 After importing data to the R environment we removed data for genes with low expression using
173 the *edgeR::filterByExpr* function (38). Normalization was then performed using the
174 *edgeR::calcNormFactors* function, and the *limma::voom* function was used to convert the data
175 into a normal distribution. We calculated differential expression using the *limma::lmFit* function
176 with empirical Bayes moderation via the *limma::eBayes* function (**Table S1**).
177
178 Several experimental conditions were applied to compare Differentially Expressed Genes
179 (DEGs) (**Table S1**). First, we compared gene expression directly between mock-infected ZAP-
180 WT and ZAP-KO Vero cells. We then used two strategies to examine transcriptional responses
181 during Zika virus infection in wild-type and knockout cells: The first strategy involved a direct

182 comparison of gene expression between Zika virus-infected ZAP-WT and ZAP-KO Vero cells.
183 The second strategy compared transcriptional responses between non-infected and infected Vero-
184 ZAP-WT cells, followed by a similar comparison between non-infected and infected Vero-ZAP-
185 KO cells. Finally, significantly affected genes (FDR < 0.05 and log2 FC > 1) were summarized
186 in **Table S2.**
187
188 Significantly affected DEGs from each experimental condition were further analyzed by
189 comparing these DEGs (**Table S2**) to a set of 194 genes involved in the interferon signaling
190 pathway. This Interferon Signaling Gene Set was obtained from Harmonizome 3.0
191 (https://maayanlab.cloud/Harmonizome/gene_set/Interferon+Signaling/Reactome+Pathways)
192 and is derived from the Reactome Pathways dataset (https://reactome.org/PathwayBrowser/#/R-
193 HSA-913531). The DEGs significantly affected in each condition that are part of the interferon
194 signaling pathway were summarized in **Table S3** and visualized in **Fig 2** for pairwise
195 comparison.
196 In addition to pairwise comparison, we performed a gene set enrichment analysis using the
197 *limma::camera* function for each experimental condition. The gene set enrichment analysis has
198 higher sensitivity than pairwise comparison because not only genes with FDR < 0.05 and $\log_2$
199 fold change (FC) > 1 (**Table S2**), but each gene in the entire input set (**Table S1)** is statistically
200 processed and used for annotation (39, 40). Gene set enrichment analysis was conducted using
201 Gene Ontology (GO) annotation for *Chlorocebus sabaeus* obtained from g:Profiler (41), and
202 significant (FDR < 0.25) GO processes for each experimental condition were summarized in
203 **Table S2**.
204

205 **Statistics**

206 Zika infectious $TCID_{50}$ titers in Vero-ZAP-WT and Vero-ZAP-KO cells were compared using an
207 unpaired t-test; $log_{10}$ transformation was performed on the $TCID_{50}$ values before the t-test. A *P*-
208 value < 0.05 was considered statistically significant.

209

210 **RESULTS**

211 Zinc finger antiviral protein (**Fig 1A; Fig S2**) affected expression of Zika virus NS5 protein, as
212 determined by Western blot at 24 h and 72 h (**Fig 1B; Fig S3**). Specifically, at 24 h post-
213 inoculation, faint Zika NS5 bands were visible in Vero-ZAP-KO cells, while the assay sensitivity
214 was insufficient to detect NS5 in Vero-ZAP-WT cells. By 72 h post-inoculation, Zika NS5 was
215 detected in both Vero-ZAP-KO and Vero-ZAP-WT cells, with protein loads considerably higher
216 in Vero-ZAP-KO cells (**Fig 1B**). In addition to NS5 Western blot, infectious Zika virus titers in
217 the supernatants of Vero-ZAP-KO cells were significantly higher than Vero-ZAP-WT titers at 48
218 and 72 hours (**Fig 1C**).

219

220

221 For RNA-seq analysis, we first compared global gene expression between mock-infected Vero-
222 ZAP-WT and Vero-ZAP-KO cells. A total of 758 and 992 genes were significantly affected and
223 differentially expressed between the two cell lines at 24 and 72 h, respectively (**Tables S2A, B**).
224 Second, we compared gene expression between Zika-infected Vero-ZAP-WT and Vero-ZAP-KO
225 cells. At 24 h, we identified 631 genes that were significantly affected and differentially
226 expressed (**Table S2E**). This number increased to 864 genes at 72 h (**Table S2F**). When we
227 compared significant DEGs between steady state (mock-infected) (**Tables S2A, B**) and Zika

228 virus-infected conditions (**Tables S2E, F**), 89 (14.1%) and 196 (22.7%) genes were uniquely
229 affected during infection at 24 h and 72 h (**Tables S2E, F**). Thus, endogenous ZAP influences
230 global gene expression both under steady-state conditions and during Zika virus infection.
231
232 Next, we compared global gene expression between mock-infected and Zika-infected Vero-ZAP-
233 WT cells. A total of 40 and 117 genes were significantly affected by infection at 24 h and 72 h
234 (**Tables S2I, J**). Finally, we compared global gene expression between mock-infected and Zika-
235 infected Vero-ZAP-KO cells. A total of 14 and 342 genes were significantly affected by
236 infection at 24 h and 72 h (**Tables S2M, N**). The higher number of significantly affected genes in
237 infected ZAP-KO cells (342 genes) compared to ZAP-WT cells (117 genes) at 72 h is not
238 surprising. This is probably because ZAP, in addition to its antiviral activity, is known to bind
239 cellular mRNA and affect gene expression leading to the resolution of antiviral and immune
240 transcriptional responses (42, 43).
241
242
243 Next, we investigated whether ZAP, beyond its impact on global gene expression, specifically
244 affects genes involved in the interferon signaling pathway. To do this, we compared significantly
245 affected DEGs in different experimental conditions (**Table S2**) with a set of 194 genes involved
246 in the interferon signaling pathway (**Table S3A**). In mock-infected Vero-ZAP-WT cells
247 compared to mock-infected Vero-ZAP-KO cells, 8 DEGs were significantly affected at 24 h and
248 11 DEGs at 72 h (**Fig 2A; Table S3B, C**). Most affected DEGs were overexpressed in Vero-
249 ZAP-WT. Interestingly, during Zika virus infection (**Fig 2B; Table S3D, E**), endogenous ZAP
250 had minimal impact on the expression of interferon signaling pathway genes because the pattern

251 of significantly affected genes in Zika virus-infected ZAP-WT and ZAP-KO cells was very
252 similar to that seen in mock-infected cells (**Fig 2A, B; Table S3B-E**). However, when
253 comparing Zika virus-infected cells to mock-infected cells, both ZAP-WT and ZAP-KO cells
254 showed increased responses to infection, including overexpression of EGR1, IFIT1, ISG15,
255 ISG20, IFIT2, OASL, ICAM1, OAS2, RSAD2, and SOCS1 (**Fig 2C, D; Table S3F-I**) which
256 were not identified by other analytical strategies (**Fig 2A, B; Table S3B-E**).

257

258 To further extend analysis beyond pairwise comparisons of top DEGs (**Fig 2; Table S3**), we
259 conducted GO analysis. This method offers high sensitivity due to its robust annotation
260 framework, standardized terminology, hierarchical structure, integration with biological
261 knowledge, continuous updates, and statistical rigor where not only genes with FDR < 0.05 and
262 $\log_2$ fold change (FC) > 1 (**Table S2**), but each gene in the entire input set (**Table S1)** is
263 statistically processed and used for annotation (39, 40).

264

265 Mock-infected Vero-ZAP-WT cells when compared to mock-infected Vero-ZAP-KO cells had
266 92 (24 h) and 178 (72 h) significantly affected GO biological processes (**Tables S2C, D**).
267 However, when we searched among affected GO biological processes keywords—"immun*"
268 and "viral/virus," we did not find affected processes containing these keywords (**Tables S2C, D**).
269 This contrasts with affected GO biological processes in infected cells described below,
270 suggesting the specificity of findings in Zika-infected cells.
271 Zika-infected Vero-ZAP-KO cells had 192 (24 h) and 481 (72 h) significantly affected GO
272 biological processes when compared to Zika-infected Vero-ZAP-WT cells (**Tables S2G, H**).
273 Zika-infected Vero-ZAP-WT cells had total 303 (24 h) and 864 (72 h) affected GO biological

274 processes as compared to mock-infected ZAP-WT cells (**Tables S2K, L**). Zika-infected Vero-
275 ZAP-KO cells had total 287 (24 h) and 384 (72 h) affected GO biological processes as compared
276 to mock-infected ZAP-WT cells (**Tables S2O, P**).
277 We narrowed down analysis and compared GO biological processes related to immune responses
278 in mock-infected Vero-ZAP-WT and Vero-ZAP-KO cells at 24 and 72 h. As expected, no
279 affected "immune*" GO processes were detected in mock-infected control cells (**Table S2C, D**).
280 After direct comparison between Zika-infected Vero-ZAP-KO and Vero-ZAP-WT cells, we
281 found one significantly affected immune process at 24 h and 72 h (**Fig 3A; Tables S2G, H**). At
282 each time point immune GO processes were upregulated in ZAP-WT cells. When compared to
283 mock-infected Vero-ZAP-WT cells, infected Vero-ZAP-WT cells showed one significantly
284 affected process at 24 h, and the number increased at 72 h reaching 16 affected processes (**Fig**
285 **3B; Tables S2K, L**). When compared to mock-infected Vero-ZAP-KO cells, infected Vero-
286 ZAP-KO cells showed one significantly affected process at 24 h, and the number increased at 72
287 h reaching only 4 affected processes (**Fig 3C; Tables S2O, P**).
288 The similar trend was observed when we narrowed down analysis and compared GO biological
289 processes related to virus infection with "viral/virus" keywords (**Tables S2C, D, G, H, K, L, O,**
290 **P**).
291

292 **DISCUSSION**

293 In a previous study, Zika virus was identified as ZAP-resistant and not sensitive to ZAP antiviral
294 activity (8). Here, we showed that ZAP acts as restriction factor for Zika virus in Vero cells.
295 Also, quantitative RNA-seq data indicated that endogenous ZAP is associated with altered global
296 gene expression both in the steady state and during Zika virus infection.

297 The previous study in A549 cells showed JEV sensitivity to ectopic and endogenous ZAP (8). In
298 the same study, Zika virus was not sensitive to ectopic ZAP; the sensitivity of Zika virus to
299 endogenous ZAP was not tested (8). Another study using ZAP wild-type and ZAP knockout A549
300 cells showed that wild-type Zika virus was also not sensitive to antiviral ZAP effects (44). Here,
301 however, we showed that Zika virus was sensitive to endogenous ZAP in Vero cells. Specifically,
302 we observed reduced infectious titers and Zika virus NS5 protein expression in wild-type cells
303 compared to ZAP knockout cells. This discrepancy may be due to the different cell lines used:
304 previous studies utilized A549 cells derived from human lung cancer tissue (8), while we used
305 Vero cells from a healthy monkey. Antiviral signaling for many cellular proteins can be highly
306 cell-specific (45). Another factor is the species difference: the previous study used a human cell
307 line, and we used an African green monkey cell line, a possible natural reservoir host of Zika virus
308 (46). Species-specific ZAP effects are documented (47, 48), but comparative studies on ZAP
309 antiviral activity between primates are lacking.
310
311 Using pairwise comparisons of DEGs, we found that endogenous ZAP impacts global gene
312 expression both in the steady state and during Zika virus infection. ZAP, however, had minimal
313 impact on the genes expression of the interferon signaling pathway. Interestingly, Zika virus
314 infection in both ZAP-WT and ZAP-KO cells was associated with increased expression of genes
315 involved in the interferon signaling pathway (**Figs 2C, D**). These findings are interesting and
316 novel in the context of Zika infection because Vero cells are deficient in IFN-α/β (4, 49). We do
317 not know yet how IFN-α/β-independent anti-Zika transcriptional responses work in Vero cells;
318 however, these responses may be attributed to type III IFN lambda. Indeed, IFN lambda 1 was
319 overexpressed in both infected ZAP-WT and ZAP-KO cells as compared to corresponding

320 mock-infected control cells at 72 h (**Table 1; Tables S2J, N**). Comparison of Zika virus-infected
321 ZAP-WT versus ZAP-KO cells suggests that ZAP may downregulate IFN lambda 1 expression
322 (FDR = 0.0005 and $\log_2$ FC = -1.006; **Table S2F**), which is supported by ability of ZAP to bind
323 cellular mRNAs and affect gene expression leading to the resolution of antiviral and immune
324 transcriptional responses (42, 43).
325 Interferon lambda induces antiviral response activating the same intracellular signaling pathways
326 and have similar biological activities as IFN-α/β, but signal via distinct receptor complex (50).
327 Also, it is known that Vero cells respond to hantavirus infection by secreting abundantly IFN
328 lambda (51), and IFN lambda protects the female reproductive tract against Zika virus infection
329 (52).
330
331 **Table 1** Interferon lambda gene expression during Zika infection in Vero-ZAP-WT and Vero-ZAP-KO cells

| | | Gene symbol | Gene name | $\log_2$ FC | FDR |
|---|---|---|---|---|---|
| ZAP-WT* | 72 h | IFNL1 | interferon lambda 1 | 4.82 | 3.83E-08 |
| ZAP-KO* | 72 h | IFNL1 | interferon lambda 1 | 5.13 | 1.52E-10 |

332 **FC**: Fold change. **FDR**: False discovery rate. Data are in **Tables S2J, N**. *IFNL1 expression during Zika infection
333 in ZAP-WT and ZAP-KO Vero cells compared to mock-infected ZAP-WT and ZAP-KO cells, respectively.
334 Direction of analysis: Zika-infected/Mock-infected.
335
336
337
338 While pairwise comparisons of DEGs showed minimal impact of ZAP on the gene expression of
339 the interferon signaling pathway, more sensitive GO analysis suggests that ZAP may augment
340 transcriptional antiviral responses. Specifically, when Zika virus-infected ZAP-KO and ZAP-WT
341 cells were compared to their corresponding mock-infected control cells, ZAP-WT infected cells
342 showed 4 times more significantly affected GO "immune" processes than ZAP-KO infected cells
343 at 72 h (16 versus 4 processes, **Fig 3B, C; Tables S2L, P**). ZAP is an IFN-stimulated gene,
344 which itself may enhance type I IFN antiviral response (1, 2, 3, 4, 5, 43, 53, 54). We do not know

345 however how ZAP may enhance type I IFN antiviral response in IFN-α/β-deficient Vero cells,
346 suggesting further research on ZAP and type III IFN interactions.
347
348
349 In this study, we used the Asian Zika virus strain, which is related to strains responsible for the
350 2015 Zika epidemic. Historical African Zika strains are known to cause more aggressive
351 infections and elicit stronger and faster innate immune responses (28, 31, 55). Previous studies
352 on Zika-ZAP interactions also used the Asian strain (8, 44). Therefore, it would be interesting to
353 conduct comparative studies to investigate how ZAP influences infections caused by both recent
354 and historical Zika strains across different cell lines.
355
356 Our study is confined to a single Vero-ZAP-KO clone, and conducting additional tests using
357 multiple clones could yield further insights. Such an endeavor falls beyond the scope of this brief
358 report; however, our RNA-seq results find indirect support from previous research conducted on
359 different uninfected wild-type and ZAP-KO cell lines. Specifically, global gene expression
360 analysis with Agilent microarrays revealed 1,065 upregulated and 776 downregulated transcripts
361 in uninfected wild-type and ZAP-KO HeLa cells (42). Another study using RNA-seq identified a
362 number of DEGs between uninfected ZAP-WT and ZAP-KO A549 cells (56). In the most recent
363 study, the authors demonstrated that ZAP influences hundreds of transcripts in ZAP-WT and
364 ZAP-KO HEK cells (57). Directly comparing the DEGs between our study and the above studies
365 poses challenges due to variations in cell types, experimental design, and the employed
366 bioinformatics. Nonetheless, the overarching trend in all previous studies strongly corroborates

367 significant transcriptional differences between uninfected ZAP-WT and ZAP-KO Vero cells
368 (**Tables S2A-D**).
369
370 The above studies did not use virus infection for RNA-seq comparison between ZAP-WT and
371 ZAP-KO cells. Thus, to our knowledge, our study provides the first high-throughput RNA-seq
372 dataset highlighting the impact of ZAP on global gene expression during virus infection, at least
373 in Vero cells. During submission of this manuscript, a study indirectly supporting our findings
374 was published (57). The authors used RNA-seq in ZAP-WT and ZAP-KO HEK cells transfected
375 with viral mimetic RNA oligos and showed that ZAP has a role in transcriptome regulation in
376 basal and antiviral states, which is in accordance with findings in the present study.
377
378
379 Altogether, we found that ZAP was associated with the inhibition of Zika virus in the absence of
380 a robust type I IFN system (Vero cells are deficient for IFN-α/β). Enrichment analysis of GO
381 processes also suggests the potential importance of ZAP in augmenting transcriptional responses
382 against Zika virus even in the absence of IFN-α/β. Further investigations are warranted to
383 elucidate the mechanisms underlying these IFN-α/β-independent antiviral cellular responses to
384 Zika virus infection, and potential antiviral interactions between ZAP and type III IFNs.
385
386
387
388
389

390 **LIST OF ABBREVIATIONS**

391 ZAP – zinc finger antiviral protein;

392 IFN – interferon;

393 WT – wild-type;

394 KO – knockout;

395 FC – fold change;

396 FDR - false discovery rate;

397 NS5 - non-structural protein 5

398 RT-qPCR - reverse transcription quantitative polymerase chain reaction;

399 $TCID_{50}$ - fifty percent tissue culture infective dose;

400 JEV - Japanese encephalitis virus;

401 YFV - yellow fever virus;

402 DENV – dengue virus;

403 HIV-1 - human immunodeficiency virus 1;

404 ZIKV – Zika virus;

405 WNV – West Nile virus.

406

407 **CONSENT FOR PUBLICATION**

408 Not applicable.

409

410 **ETHICS APPROVAL AND CONSENT TO PARTICIPATE**

411 Not applicable.

412

## AVAILABILITY OF DATA AND MATERIALS

Data are provided within the manuscript or supplementary information files. Raw RNA-seq files are deposited to NCBI BioProject (PRJNA1101086).

## COMPETING INTERESTS

The authors declare that they have no competing interests.


## FUNDING

PPS received a Scholarship from the School of Public Health, University of Saskatchewan. This work was partially supported by a grant to UK from the Canadian Institutes of Health Research (CIHR; Project Grant #424307). The funders had no role in study design, data collection and analysis, decision to publish, or manuscript preparation.


## AUTHORS' CONTRIBUTIONS

Conceptualization: UK. Investigation: NPKL, PPS, AJS, UK. Data analysis: NPKL, PPS, IT, UK. Funding: UK. Resources: UK. Writing—original draft preparation: NPKL, UK. Writing—review and editing: UK, NPKL, IT, PPS.

436 **REFERENCES**


437 1. Nguyen LP, Aldana KS, Yang E, Yao Z, Li MMH. Alphavirus Evasion of Zinc Finger Antiviral Protein
438 (ZAP) Correlates with CpG Suppression in a Specific Viral nsP2 Gene Sequence. Viruses. 2023;15(4).
439 2. MacDonald MR, Machlin ES, Albin OR, Levy DE. The zinc finger antiviral protein acts
440 synergistically with an interferon-induced factor for maximal activity against alphaviruses. J Virol.
441 2007;81(24):13509-18.
442 3. Li MMH, Aguilar EG, Michailidis E, Pabon J, Park P, Wu X, et al. Characterization of Novel Splice
443 Variants of Zinc Finger Antiviral Protein (ZAP). J Virol. 2019;93(18).
444 4. Crosse KM, Monson EA, Beard MR, Helbig KJ. Interferon-Stimulated Genes as Enhancers of
445 Antiviral Innate Immune Signaling. J Innate Immun. 2018;10(2):85-93.
446 5. Hayakawa S, Shiratori S, Yamato H, Kameyama T, Kitatsuji C, Kashigi F, et al. ZAPS is a potent
447 stimulator of signaling mediated by the RNA helicase RIG-I during antiviral responses. Nat Immunol.
448 2011;12(1):37-44.
449 6. Takata MA, Goncalves-Carneiro D, Zang TM, Soll SJ, York A, Blanco-Melo D, et al. CG
450 dinucleotide suppression enables antiviral defence targeting non-self RNA. Nature. 2017;550(7674):124-
451 7.
452 7. Zhu Y, Gao G. ZAP-mediated mRNA degradation. RNA Biol. 2008;5(2):65-7.
453 8. Chiu HP, Chiu H, Yang CF, Lee YL, Chiu FL, Kuo HC, et al. Inhibition of Japanese encephalitis virus
454 infection by the host zinc-finger antiviral protein. PLoS Pathogens: Public Library of Science; 2018.
455 9. Ye P, Liu S, Zhu Y, Chen G, Gao G. DEXH-Box protein DHX30 is required for optimal function of
456 the zinc-finger antiviral protein. Protein Cell. 2010;1(10):956-64.
457 10. Chen G, Guo X, Lv F, Xu Y, Gao G. p72 DEAD box RNA helicase is required for optimal function of
458 the zinc-finger antiviral protein. Proc Natl Acad Sci U S A. 2008;105(11):4352-7.
459 11. Li MM, Lau Z, Cheung P, Aguilar EG, Schneider WM, Bozzacco L, et al. TRIM25 Enhances the
460 Antiviral Action of Zinc-Finger Antiviral Protein (ZAP). PLoS Pathog. 2017;13(1):e1006145.
461 12. Zheng X, Wang X, Tu F, Wang Q, Fan Z, Gao G. TRIM25 Is Required for the Antiviral Activity of
462 Zinc Finger Antiviral Protein. Journal of virology: J Virol; 2017.
463 13. Ficarelli M, Wilson H, Pedro Galão R, Mazzon M, Antzin-Anduetza I, Marsh M, et al. KHNYN is
464 essential for the zinc finger antiviral protein (ZAP) to restrict HIV-1 containing clustered CpG
465 dinucleotides. eLife2019.
466 14. Buckmaster MV, Goff SP. Riplet Binds the Zinc Finger Antiviral Protein (ZAP) and Augments ZAP-
467 Mediated Restriction of HIV-1. Journal of Virology: American Society for Microbiology; 2022.
468 15. Gao G, Guo X, Goff SP. Inhibition of retroviral RNA production by ZAP, a CCCH-type zinc finger
469 protein. Science (New York, NY): American Association for the Advancement of Science; 2002. p. 1703-6.
470 16. Bick MJ, Carroll JW, Gao G, Goff SP, Rice CM, MacDonald MR. Expression of the zinc-finger
471 antiviral protein inhibits alphavirus replication. J Virol. 2003;77(21):11555-62.
472 17. Liu CH, Zhou L, Chen G, Krug RM. Battle between influenza A virus and a newly identified
473 antiviral activity of the PARP-containing ZAPL protein. Proc Natl Acad Sci U S A. 2015;112(45):14048-53.
474 18. Mao R, Nie H, Cai D, Zhang J, Liu H, Yan R, et al. Inhibition of hepatitis B virus replication by the
475 host zinc finger antiviral protein. PLoS Pathog. 2013;9(7):e1003494.
476 19. Muller S, Moller P, Bick MJ, Wurr S, Becker S, Gunther S, et al. Inhibition of filovirus replication
477 by the zinc finger antiviral protein. J Virol. 2007;81(5):2391-400.
478 20. Tang Q, Wang X, Gao G. The Short Form of the Zinc Finger Antiviral Protein Inhibits Influenza A
479 Virus Protein Expression and Is Antagonized by the Virus-Encoded NS1. J Virol. 2017;91(2).
480 21. Zhu Y, Chen G, Lv F, Wang X, Ji X, Xu Y, et al. Zinc-finger antiviral protein inhibits HIV-1 infection
481 by selectively targeting multiply spliced viral mRNAs for degradation. Proc Natl Acad Sci U S A.
482 2011;108(38):15834-9.

483 22. Miyazato P, Matsuo M, Tan BJY, Tokunaga M, Katsuya H, Islam S, et al. HTLV-1 contains a high
484 CG dinucleotide content and is susceptible to the host antiviral protein ZAP. Retrovirology.
485 2019;16(1):38.
486 23. Gonzalez-Perez AC, Stempel M, Wyler E, Urban C, Piras A, Hennig T, et al. The Zinc Finger
487 Antiviral Protein ZAP Restricts Human Cytomegalovirus and Selectively Binds and Destabilizes Viral
488 UL4/UL5 Transcripts. mBio. 2021;12(3).
489 24. Zhao Y, Song Z, Bai J, Liu X, Nauwynck H, Jiang P. ZAP, a CCCH-Type Zinc Finger Protein, Inhibits
490 Porcine Reproductive and Respiratory Syndrome Virus Replication and Interacts with Viral Nsp9. J Virol.
491 2019;93(10).
492 25. Xie L, Lu B, Zheng Z, Miao Y, Liu Y, Zhang Y, et al. The 3C protease of enterovirus A71 counteracts
493 the activity of host zinc-finger antiviral protein (ZAP). J Gen Virol. 2018;99(1):73-85.
494 26. Trus I, Udenze D, Berube N, Wheler C, Martel MJ, Gerdts V, et al. CpG-Recoding in Zika Virus
495 Genome Causes Host-Age-Dependent Attenuation of Infection With Protection Against Lethal
496 Heterologous Challenge in Mice. Front Immunol. 2019;10:3077.
497 27. Trus I, Berube N, Jiang P, Rak J, Gerdts V, Karniychuk U. Zika Virus with Increased CpG
498 Dinucleotide Frequencies Shows Oncolytic Activity in Glioblastoma Stem Cells. Viruses: Multidisciplinary
499 Digital Publishing Institute; 2020. p. 579.
500 28. Udenze D, Trus I, Berube N, Gerdts V, Karniychuk U. The African strain of Zika virus causes more
501 severe in utero infection than Asian strain in a porcine fetal transmission model. Emerging Microbes &
502 Infections 2019; 8:1098-11072019.
503 29. Darbellay J, Cox B, Lai K, Delgado-Ortega M, Wheler C, Wilson D, et al. Zika Virus Causes
504 Persistent Infection in Porcine Conceptuses and may Impair Health in Offspring. EBioMedicine 25:73-
505 862017.
506 30. Chapagain S, Pal Singh P, Le K, Safronetz D, Wood H, Karniychuk U. Japanese encephalitis virus
507 persists in the human reproductive epithelium and porcine reproductive tissues. PLoS Negl Trop Dis.
508 2022;16(7):e0010656.
509 31. Sabir AJ, Singh PP, Trus I, Le NPK, Karniychuk U. Asian Zika virus can acquire generic African-
510 lineage mutations during in utero infection. Emerg Microbes Infect. 2023;12(2):2263592.
511 32. Darbellay J, Lai K, Babiuk S, Berhane Y, Ambagala A, Wheler C, et al. Neonatal pigs are
512 susceptible to experimental Zika virus infection. Emerg Microbes Infect. 2017;6(2):e6.
513 33. Trus I, Udenze D, Cox B, Berube N, Nordquist RE, van der Staay FJ, et al. Subclinical in utero Zika
514 virus infection is associated with interferon alpha sequelae and sex-specific molecular brain pathology in
515 asymptomatic porcine offspring. In: Pierson TC, editor. PLoS Pathogens2019. p. e1008038.
516 34. Xu MY, Liu SQ, Deng CL, Zhang QY, Zhang B. Detection of Zika virus by SYBR green one-step real-
517 time RT-PCR. Journal of virological methods: J Virol Methods; 2016. p. 93-7.
518 35. Udenze D, Trus I, Lipsit S, Napper S, Karniychuk U. Offspring affected with in utero Zika virus
519 infection retain molecular footprints in the bone marrow and blood cells. Emerging microbes &
520 infections: Emerg Microbes Infect; 2022. p. 1-43.
521 36. Bray NL, Pimentel H, Melsted P, Pachter L. Near-optimal probabilistic RNA-seq quantification.
522 Nature Biotechnology. 2016;34(5):525-7.
523 37. Warren WC, Jasinska AJ, Garcia-Perez R, Svardal H, Tomlinson C, Rocchi M, et al. The genome of
524 the vervet (Chlorocebus aethiops sabaeus). Genome Res. 2015;25(12):1921-33.
525 38. Law CW, Alhamdoosh M, Su S, Dong X, Tian L, Smyth GK, et al. RNA-seq analysis is easy as 1-2-3
526 with limma, Glimma and edgeR. F1000Res. 2016;5.
527 39. The Gene Ontology C. The Gene Ontology Resource: 20 years and still GOing strong. Nucleic
528 Acids Res. 2019;47(D1):D330-D8.
529 40. Ashburner M, Ball CA, Blake JA, Botstein D, Butler H, Cherry JM, et al. Gene ontology: tool for
530 the unification of biology. The Gene Ontology Consortium. Nat Genet. 2000;25(1):25-9.

531 41. Raudvere U, Kolberg L, Kuzmin I, Arak T, Adler P, Peterson H, et al. g:Profiler: a web server for
532 functional enrichment analysis and conversions of gene lists (2019 update). Nucleic Acids Res.
533 2019;47(W1):W191-W8.
534 42. Todorova T, Bock FJ, Chang P. PARP13 regulates cellular mRNA post-transcriptionally and
535 functions as a pro-apoptotic factor by destabilizing TRAILR4 transcript. Nat Commun. 2014;5:5362.
536 43. Schwerk J, Soveg FW, Ryan AP, Thomas KR, Hatfield LD, Ozarkar S, et al. RNA-binding protein
537 isoforms ZAP-S and ZAP-L have distinct antiviral and immune resolution functions. Nat Immunol.
538 2019;20(12):1610-20.
539 44. Fros JJ, Visser I, Tang B, Yan K, Nakayama E, Visser TM, et al. The dinucleotide composition of the
540 Zika virus genome is shaped by conflicting evolutionary pressures in mammalian hosts and mosquito
541 vectors. PLoS Biol. 2021;19(4):e3001201.
542 45. Pallett MA, Lu Y, Smith GL. DDX50 Is a Viral Restriction Factor That Enhances IRF3 Activation.
543 Viruses. 2022;14(2).
544 46. Buechler CR, Bailey AL, Weiler AM, Barry GL, Breitbach ME, Stewart LM, et al. Seroprevalence of
545 Zika Virus in Wild African Green Monkeys and Baboons. mSphere. 2017;2(2).
546 47. Kerns JA, Emerman M, Malik HS. Positive selection and increased antiviral activity associated
547 with the PARP-containing isoform of human zinc-finger antiviral protein. PLoS Genet. 2008;4(1):e21.
548 48. Goncalves-Carneiro D, Takata MA, Ong H, Shilton A, Bieniasz PD. Origin and evolution of the zinc
549 finger antiviral protein. PLoS Pathog. 2021;17(4):e1009545.
550 49. Emeny JM, Morgan MJ. Regulation of the interferon system: evidence that Vero cells have a
551 genetic defect in interferon production. J Gen Virol. 1979;43(1):247-52.
552 50. Lopusna K, Rezuchova I, Kabat P, Kudelova M. Interferon lambda induces antiviral response to
553 herpes simplex virus 1 infection. Acta Virol. 2014;58(4):325-32.
554 51. Prescott J, Hall P, Acuna-Retamar M, Ye C, Wathelet MG, Ebihara H, et al. New World
555 hantaviruses activate IFNlambda production in type I IFN-deficient vero E6 cells. PLoS One.
556 2010;5(6):e11159.
557 52. Caine EA, Scheaffer SM, Arora N, Zaitsev K, Artyomov MN, Coyne CB, et al. Interferon lambda
558 protects the female reproductive tract against Zika virus infection. Nature Communications 2019 10:1:
559 Nature Publishing Group; 2019. p. 1-12.
560 53. Lee H, Komano J, Saitoh Y, Yamaoka S, Kozaki T, Misawa T, et al. Zinc-finger antiviral protein
561 mediates retinoic acid inducible gene I-like receptor-independent antiviral response to murine leukemia
562 virus. Proc Natl Acad Sci U S A. 2013;110(30):12379-84.
563 54. Kozaki T, Takahama M, Misawa T, Matsuura Y, Akira S, Saitoh T. Role of zinc-finger anti-viral
564 protein in host defense against Sindbis virus. Int Immunol. 2015;27(7):357-64.
565 55. Esser-Nobis K, Aarreberg LD, Roby JA, Fairgrieve MR, Green R, Gale M, Jr. Comparative Analysis
566 of African and Asian Lineage-Derived Zika Virus Strains Reveals Differences in Activation of and
567 Sensitivity to Antiviral Innate Immunity. J Virol. 2019;93(13).
568 56. Shaw AE, Rihn SJ, Mollentze N, Wickenhagen A, Stewart DG, Orton RJ, et al. The antiviral state
569 has shaped the CpG composition of the vertebrate interferome to avoid self-targeting. PLoS Biol.
570 2021;19(9):e3001352.
571 57. Busa VF, Ando Y, Aigner S, Yee BA, Yeo GW, Leung AKL. Transcriptome regulation by PARP13 in
572 basal and antiviral states in human cells. iScience. 2024;27(4):109251.

573

574

575 **FIGURE LEGENDS**

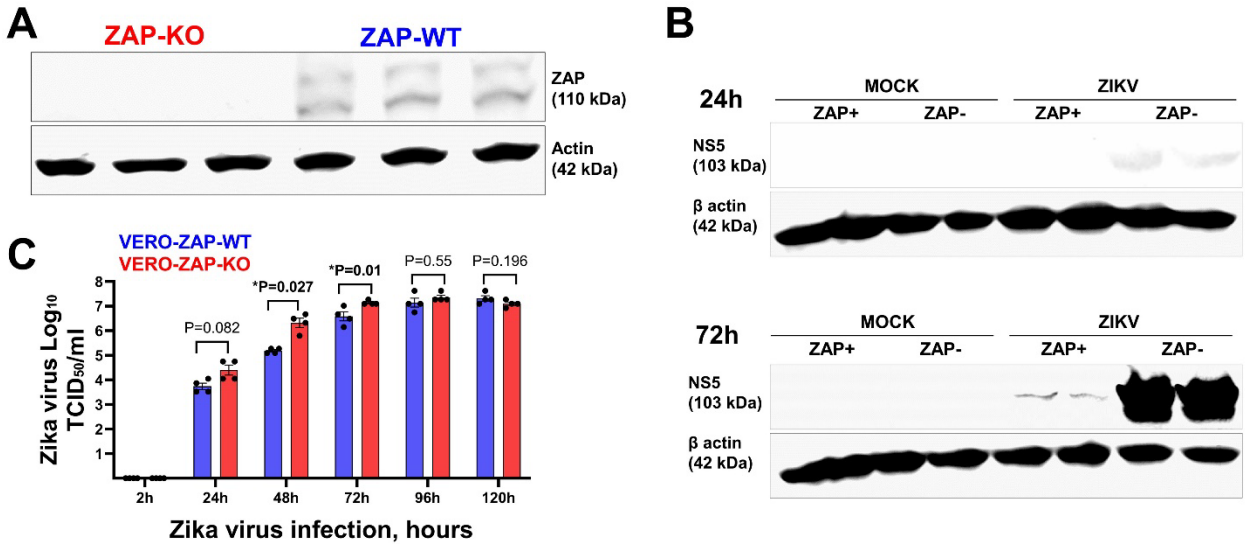


576

577 **Fig 1. Infection phenotypes of Zika virus in wild-type (Vero-ZAP-WT) and ZAP knockout**
578 **(Vero-ZAP-KO) cells.** (**A**) ZAP Western blot. KO status was also confirmed by Sanger
579 sequencing. Rabbit anti-ZAP IgG Abs (1:1,000 dilution; ANTI-ZC3HAV1; #HPA059096-
580 100UL, Sigma-Aldrich), with the specific ZAP band appearing at 110 kDa, were used. Beta-
581 actin was used as a western blot loading control (42 kDa). A normalized 50 µg of protein was
582 used for all samples. Three replicates. Multiple bands may represent isoforms described for
583 human ZAP (3) and still not experimentally characterized for monkeys. The full blot image is in
584 **Figure S2**. (**B**) Zika virus NS5 protein Western blot. Reduced Zika virus NS5 protein loads in
585 Vero-ZAP-WT cells as compared to Vero-ZAP-KO cells at 24 h and 72 h after inoculation, MOI
586 1. Rabbit anti-Zika virus NS5 IgG Abs (1:1,000 dilution; GTX133312, GeneTex), with the
587 specific NS5 band appearing at 103 kDa, were used. Beta-actin was used as a western blot
588 loading control (42 kDa). A normalized 50 µg of protein was used for all samples. Two
589 biological replicates for each condition are shown. The full blot image is in **Figure S3**. (**C**) Zika
590 virus infectious titers in supernatants of Vero-ZAP-WT and Vero-ZAP-KO cells at different
591 times after inoculation, MOI 1. The experiment was done in four replicates for each cell line and
592 sampling time. Supernatants from all mock-infected samples were negative. Statistics—an
593 unpaired t-test. *A P-value of < 0.05 was considered statistically significant.

594
595
596
597
598
599

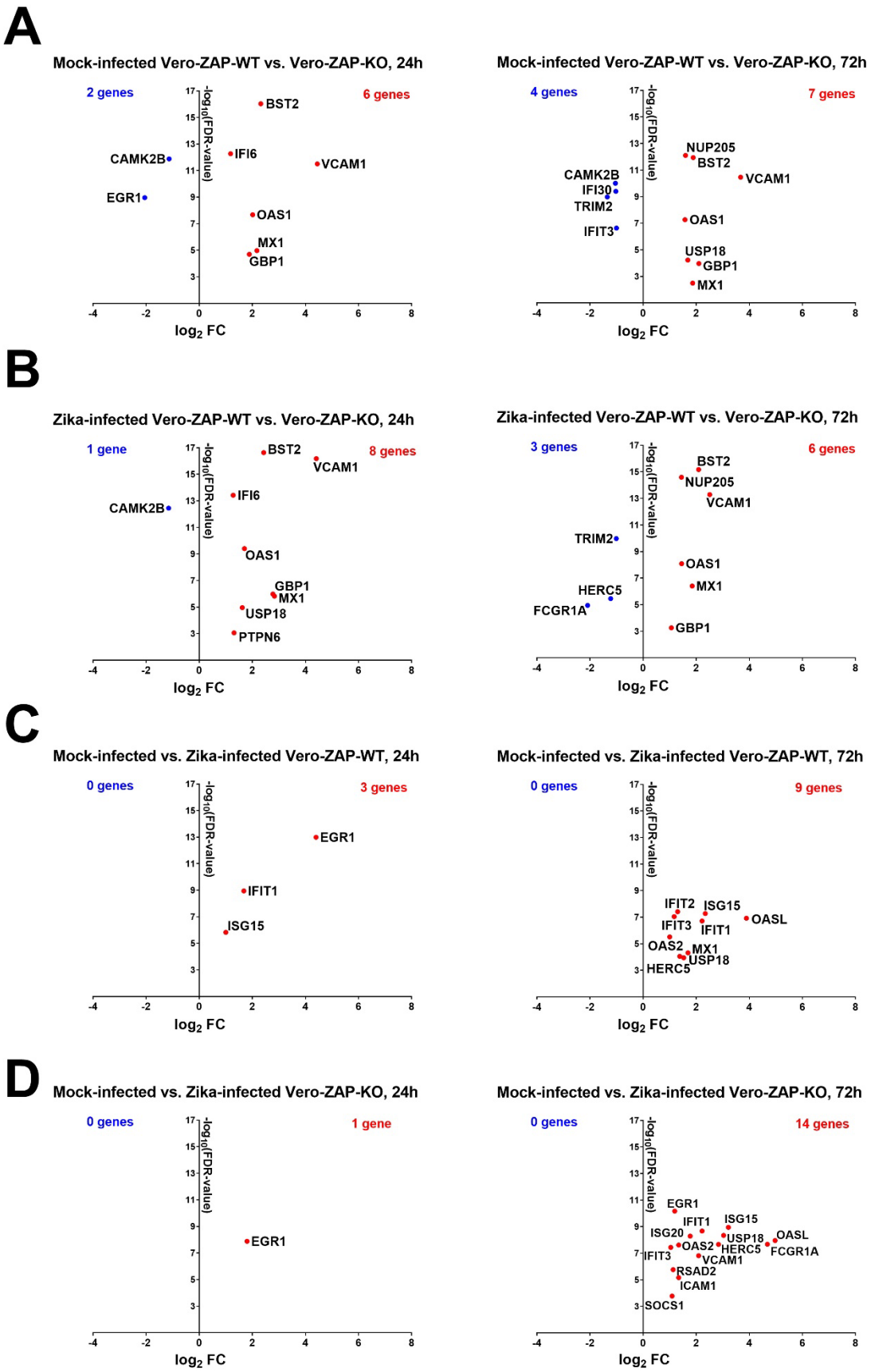
A
Mock-infected Vero-ZAP-WT vs. Vero-ZAP-KO, 24h
2 genes
6 genes
BST2
IFI6
CAMK2B
VCAM1
EGR1
OAS1
MX1
GBP1
Mock-infected Vero-ZAP-WT vs. Vero-ZAP-KO, 72h
4 genes
7 genes
NUP205
BST2
CAMK2B
VCAM1
IFI30
TRIM2
OAS1
IFIT3
USP18
GBP1
MX1
B
Zika-infected Vero-ZAP-WT vs. Vero-ZAP-KO, 24h
1 gene
8 genes
BST2
VCAM1
IFI6
CAMK2B
OAS1
GBP1
MX1
USP18
PTPN6
Zika-infected Vero-ZAP-WT vs. Vero-ZAP-KO, 72h
3 genes
6 genes
BST2
NUP205
VCAM1
TRIM2
OAS1
MX1
HERC5
FCGR1A
GBP1
C
Mock-infected vs. Zika-infected Vero-ZAP-WT, 24h
0 genes
3 genes
EGR1
IFIT1
ISG15
Mock-infected vs. Zika-infected Vero-ZAP-WT, 72h
0 genes
9 genes
IFIT2
ISG15
OASL
IFIT3
IFIT1
OAS2
MX1
USP18
HERC5
D
Mock-infected vs. Zika-infected Vero-ZAP-KO, 24h
0 genes
1 gene
EGR1
Mock-infected vs. Zika-infected Vero-ZAP-KO, 72h
0 genes
14 genes
EGR1
IFIT1
ISG15
ISG20
OAS2
USP18
OASL
HERC5
FCGR1A
IFIT3
VCAM1
RSAD2
ICAM1
SOCS1
-log10(FDR-value)
log2 FC

600

601 **Fig 2. Significantly affected interferon signaling genes in different experimental conditions.**
602 (**A**) Mock-infected Vero-ZAP-WT versus Vero-ZAP-KO cells. Direction of analysis: WT/KO.
603 **Tables S3B, C**. (**B**) Zika-infected Vero-ZAP-WT versus Vero-ZAP-KO cells. Direction of
604 analysis: WT/KO. **Tables S3D, E.** (**C**) Mock-infected versus Zika-infected Vero-ZAP-WT cells.
605 Direction of analysis: Zika-infected/Mock-infected. **Tables S3F, G.** (**D**) Mock-infected versus
606 Zika-infected Vero-ZAP-KO cells. Direction of analysis: Zika-infected/Mock-infected. **Tables**
607 **S3H, I.** Plots of the upregulated (red) and downregulated (blue) genes. **FDR**: The false discovery
608 rate. Genes with FDR < 0.05 and $\log_2$ fold change (FC) > 1 were significantly affected.
609
610
611
612
613
614
615
616
617
618
619
620
621
622
623
624
625
626

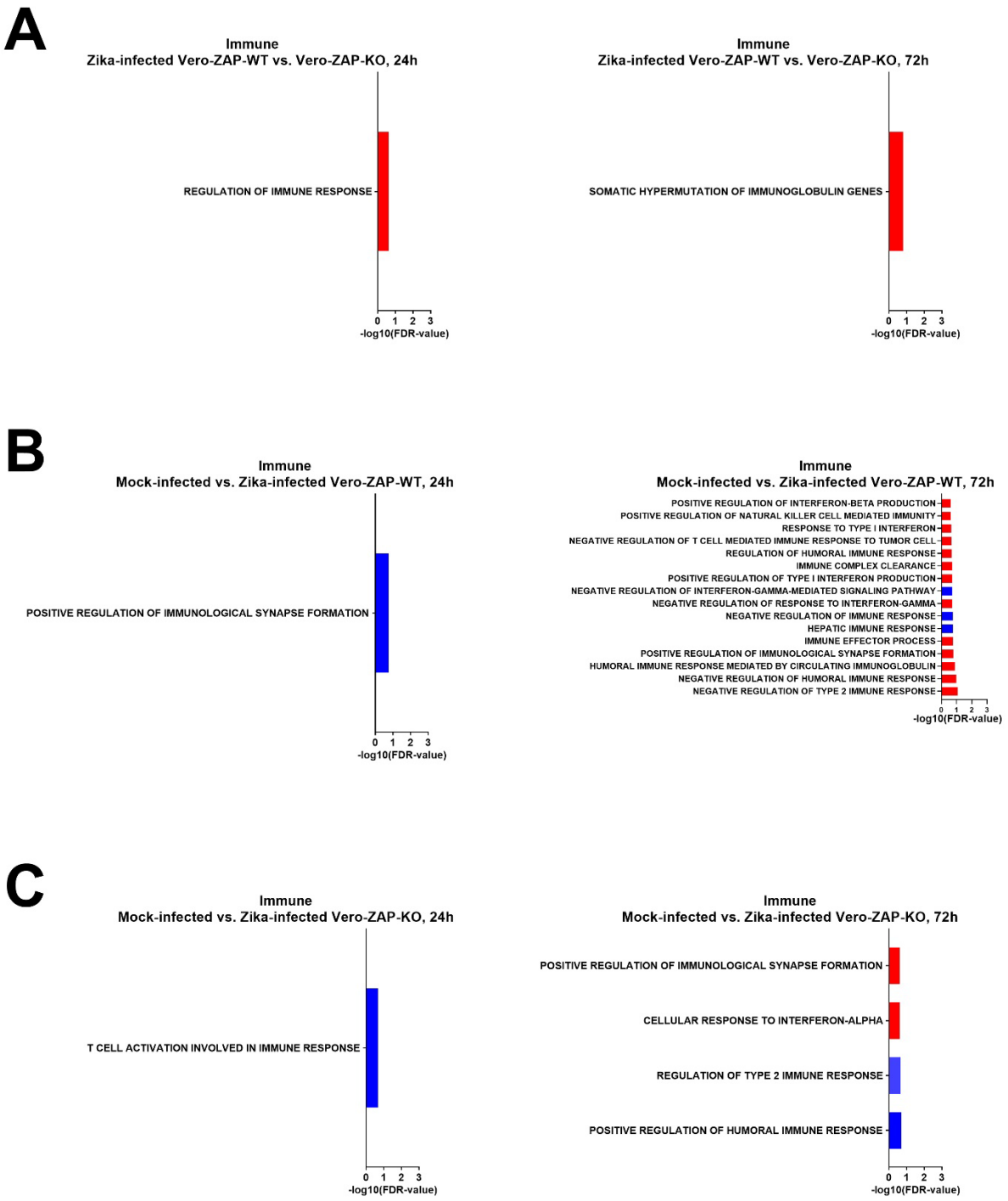


**Fig 3. Biological "immune*" processes significantly affected in Vero-ZAP-WT and Vero-ZAP-KO cells at 24 h and 72 h after Zika virus infection.** (**A**) Zika-infected Vero-ZAP-WT versus Vero-ZAP-KO cells. Direction of analysis: WT/KO. **Tables S2G, H.** (**B**) Mock-infected versus Zika-infected Vero-ZAP-WT cells. Direction of analysis: Zika-infected/Mock-infected. **Tables S2K, L.** (**C**) Mock-infected versus Zika-infected Vero-ZAP-KO cells. Direction of analysis: Zika-infected/Mock-infected. **Tables S2O, P.** Red bars–upregulated processes. Blue bars– downregulated processes. **FDR**: The false discovery rate.

635 **SUPPLEMENTARY TABLES**

636

637 **Table S1** Raw RNAseq data (DEGs).

638

639 **Table S2** Significantly affected DEGs and GO processes.

640

641 **Table S3** Expression of Interferon Signaling Genes in different experimental conditions.

642

643 **Fig S1. CpG dinucleotide content in flavivirus genomes.** The bar plot is the CpG frequency in
644 the whole flavivirus RNA genomes (the ratio of observed and arithmetically expected CpG
645 dinucleotides determined by SSE 1.4 software). Line graphs show the number of CpG
646 dinucleotides within the RNA genome with a 50 nt sliding window. Calculations were made with
647 an R script (https://github.com/itrus/Mapping-ROIs-in-genetic-sequences/blob/main/CpG-map-
648 linear.R). **JEV**—Japanese Encephalitis virus (GenBank: MK585066.1 reference genome);
649 **ZIKV**—Zika virus (GenBank: KJ776791.2); **DENV**—dengue virus (GenBank: U87411.1);
650 **YFV**—yellow fever virus (GenBank: X03700.1); **WNV**—West Nile virus (GenBank:
651 DQ211652.1).

652

653 **Fig S2. ZAP Western blot.** The full blot image. Rabbit anti-ZAP IgG Abs (1:1,000 dilution;
654 ANTI-ZC3HAV1; #HPA059096-100UL, Sigma-Aldrich), with the specific ZAP band appearing
655 at 110 kDa, were used. Multiple bands may represent four isoforms described for human ZAP
656 (3) and still not experimentally characterized for monkeys.

657

658 **Fig S3. Zika virus NS5 Western blot.** The full blot image. Rabbit anti-Zika virus NS5 IgG Abs
659 (1:1,000 dilution; GTX133312, GeneTex), with the specific NS5 band appearing at 103 kDa,
660 were used.

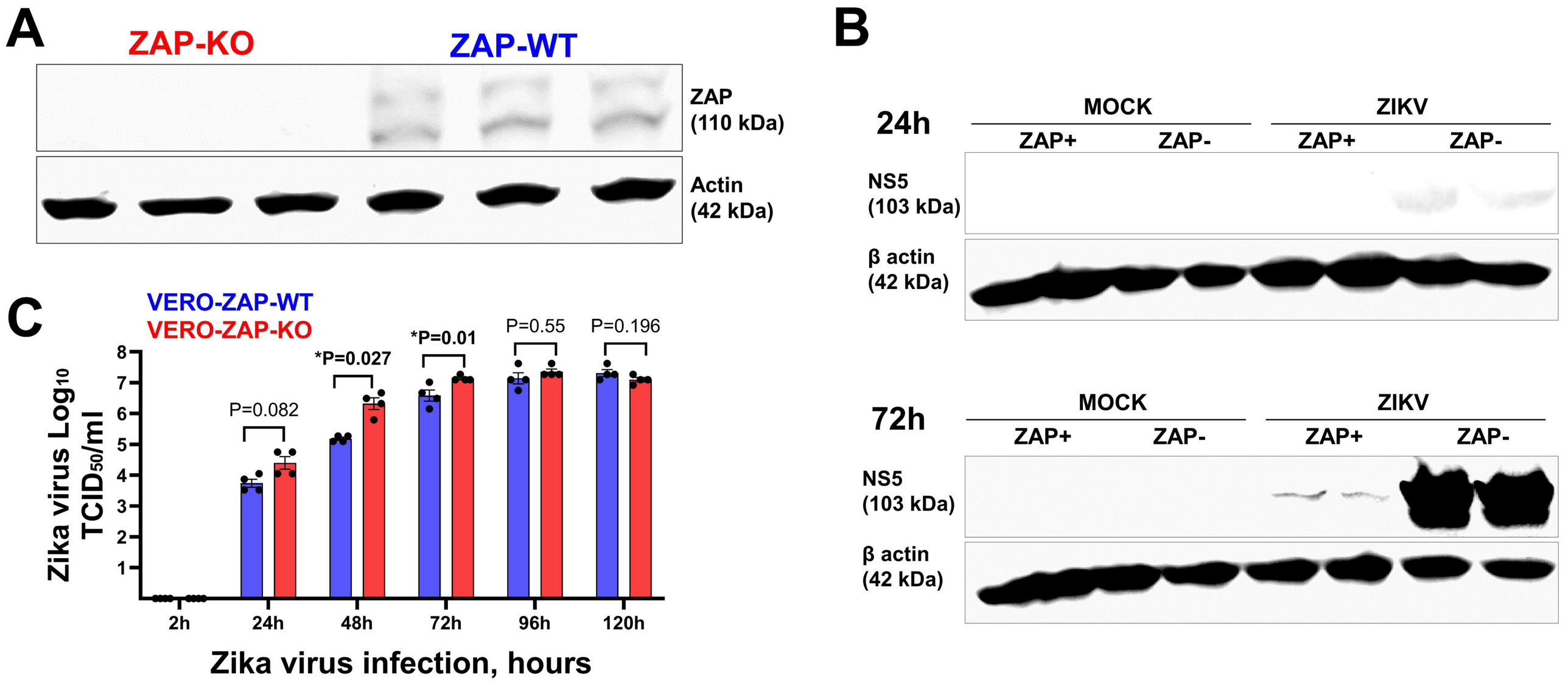
A
ZAP-KO
ZAP-WT
ZAP
(110 kDa)
Actin
(42 kDa)
B
24h
MOCK
ZIKV
ZAP+
ZAP-
ZAP+
ZAP-
NS5
(103 kDa)
β actin
(42 kDa)
72h
MOCK
ZIKV
ZAP+
ZAP-
ZAP+
ZAP-
NS5
(103 kDa)
β actin
(42 kDa)
C
VERO-ZAP-WT
VERO-ZAP-KO
P=0.082
*P=0.027
*P=0.01
P=0.55
P=0.196
Zika virus Log10 TCID50/ml
8
7
6
5
4
3
2
1
2h
24h
48h
72h
96h
120h
Zika virus infection, hours

# A

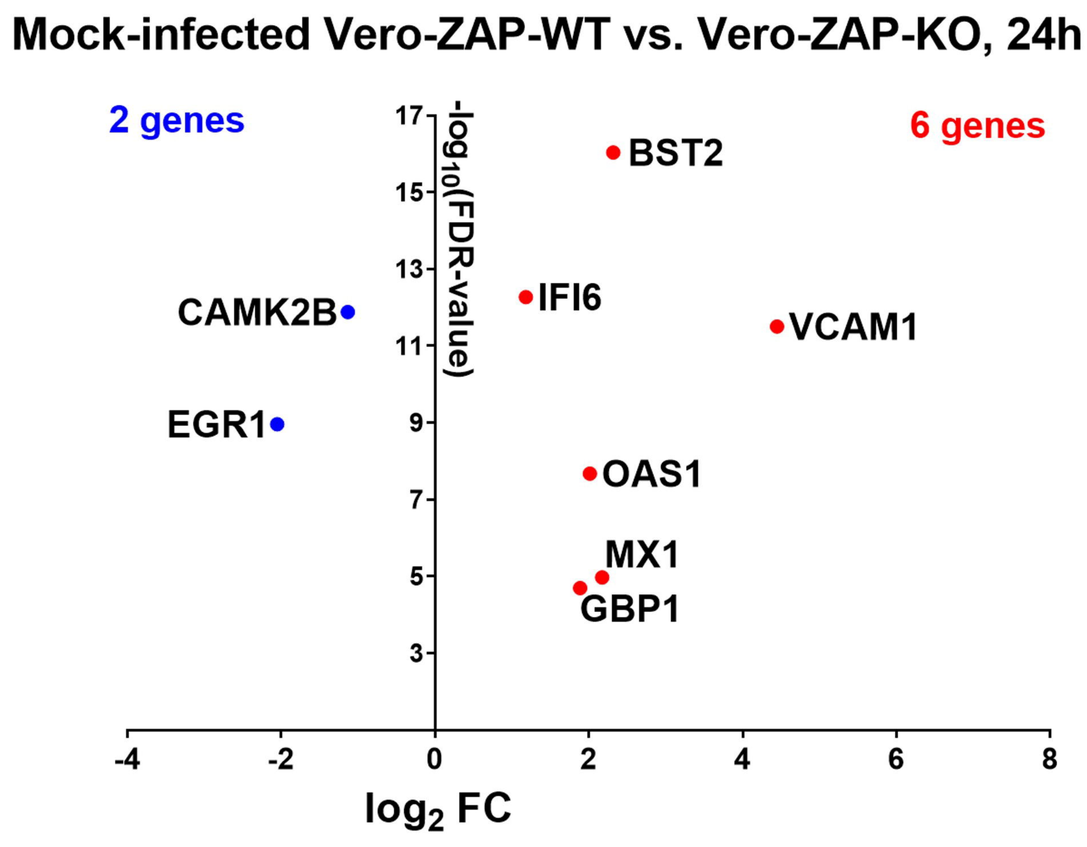
Mock-infected Vero-ZAP-WT vs. Vero-ZAP-KO, 24h
2 genes
6 genes
BST2
CAMK2B
IFI6
VCAM1
EGR1
OAS1
MX1
GBP1
-log10(FDR-value)
log2 FC

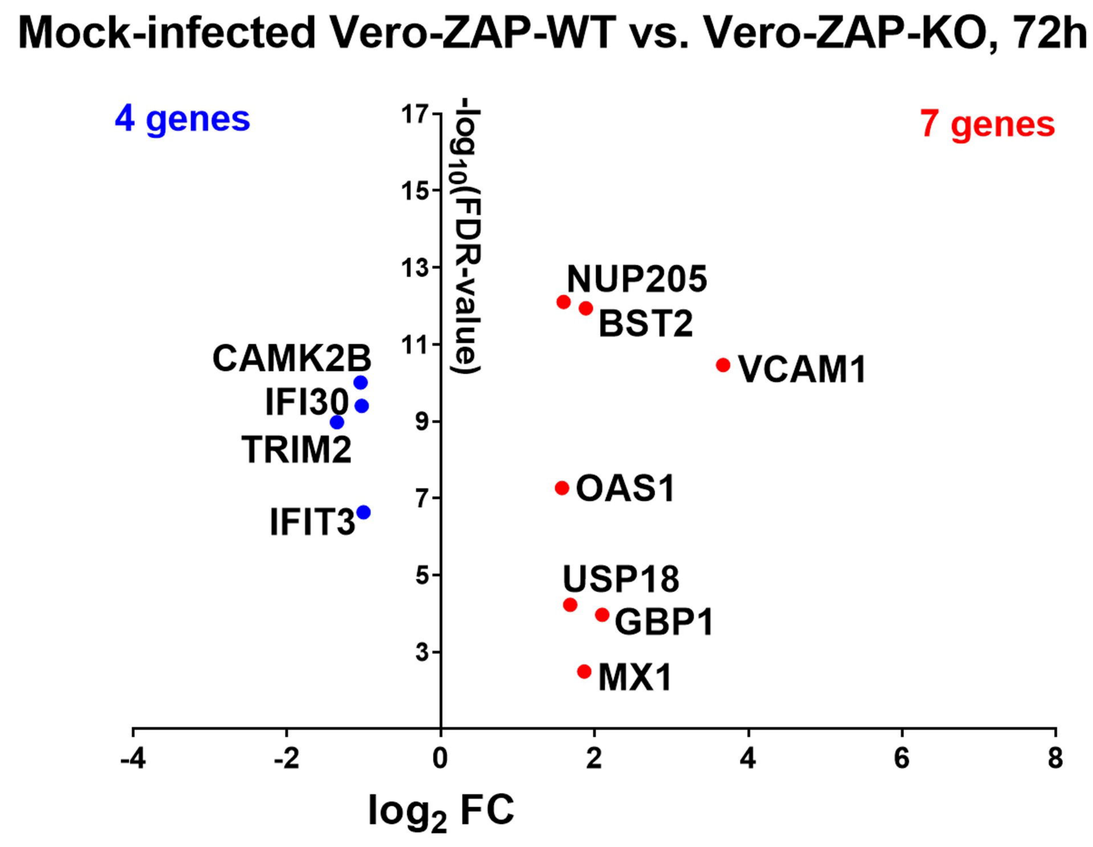
Mock-infected Vero-ZAP-WT vs. Vero-ZAP-KO, 72h
4 genes
7 genes
NUP205
BST2
CAMK2B
IFI30
TRIM2
VCAM1
OAS1
IFIT3
USP18
GBP1
MX1
-log10(FDR-value)
log2 FC

# B

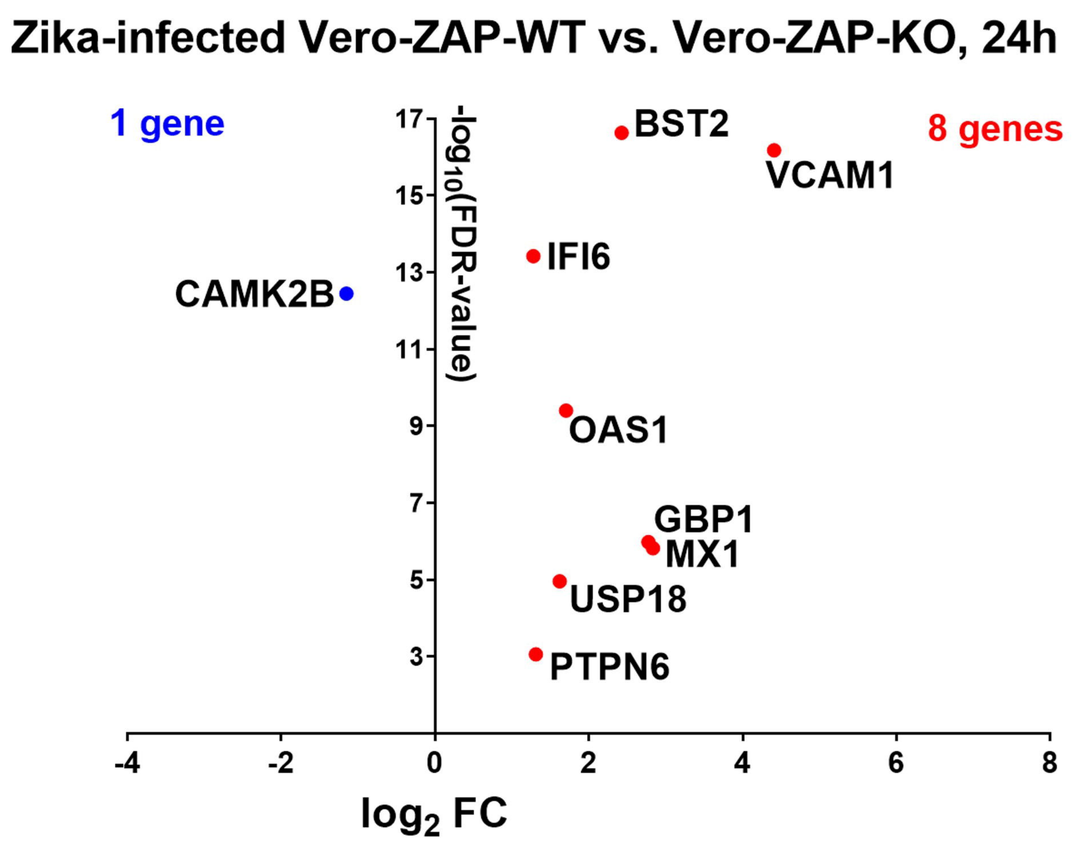
Zika-infected Vero-ZAP-WT vs. Vero-ZAP-KO, 24h
1 gene
8 genes
BST2
VCAM1
IFI6
CAMK2B
OAS1
GBP1
MX1
USP18
PTPN6
-log10(FDR-value)
log2 FC

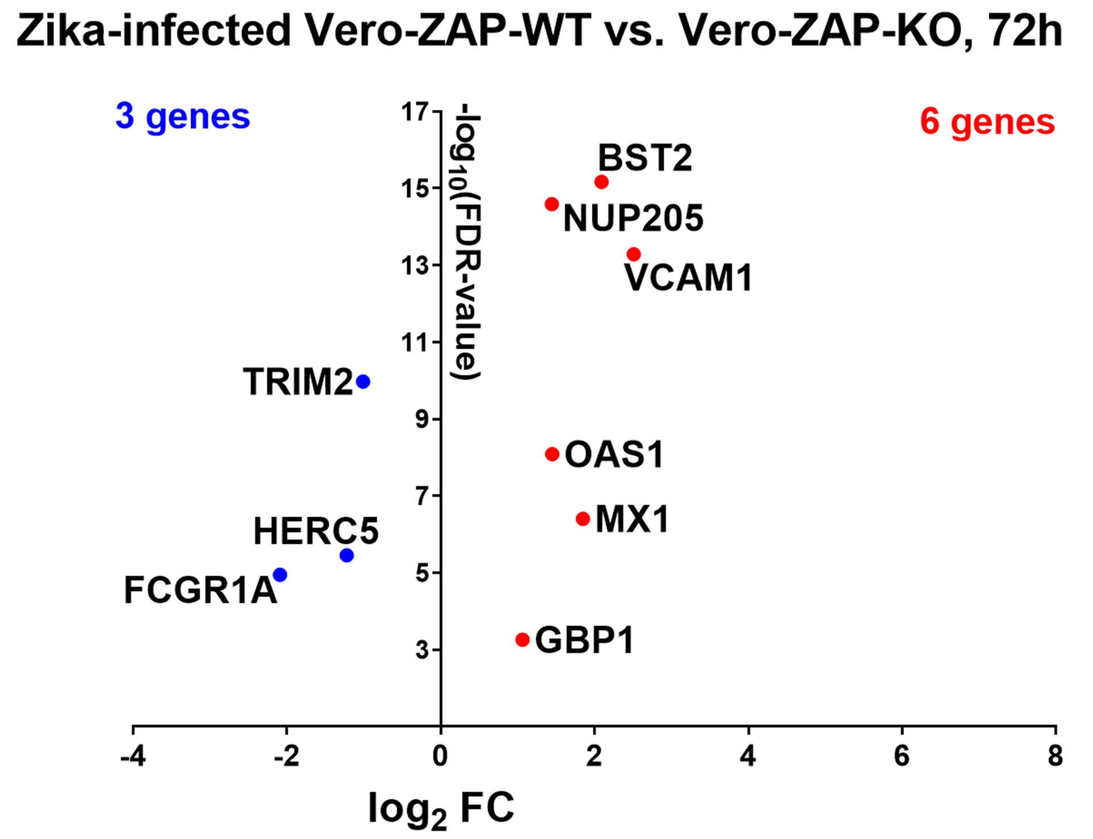
Zika-infected Vero-ZAP-WT vs. Vero-ZAP-KO, 72h
3 genes
6 genes
BST2
NUP205
VCAM1
TRIM2
OAS1
MX1
HERC5
FCGR1A
GBP1
-log10(FDR-value)
log2 FC

# C

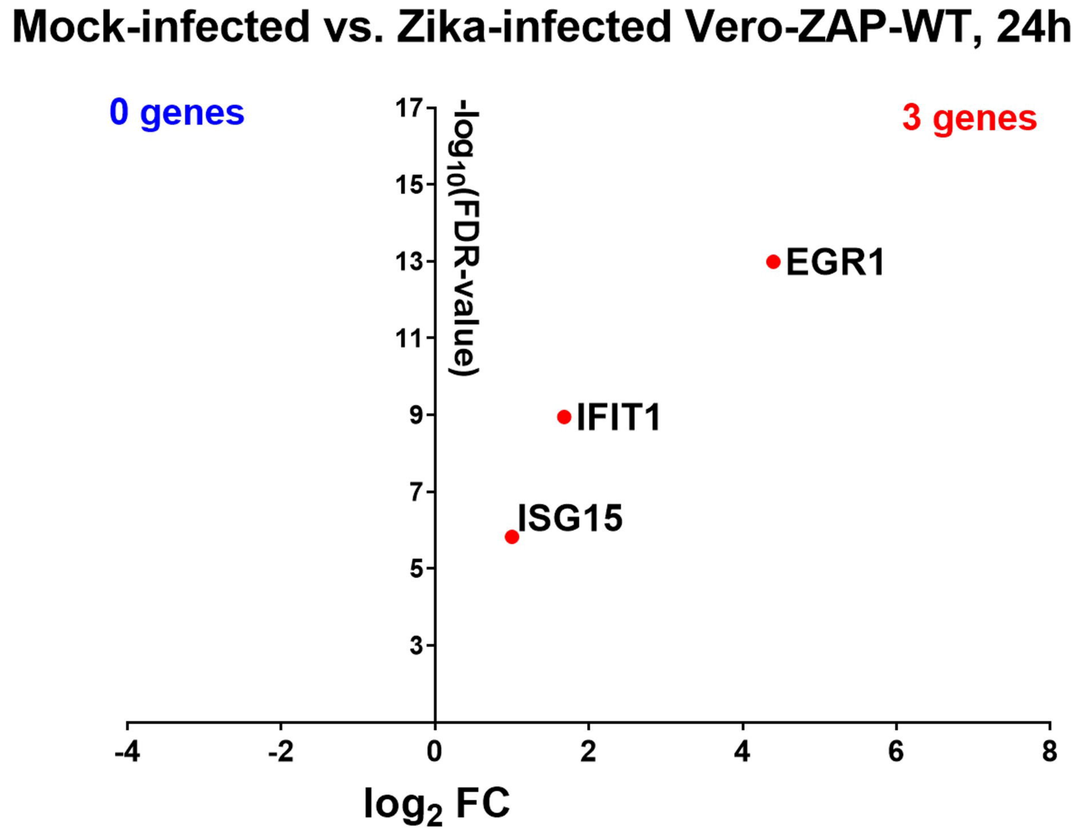
Mock-infected vs. Zika-infected Vero-ZAP-WT, 24h
0 genes
3 genes
EGR1
IFIT1
ISG15
-log10(FDR-value)
log2 FC

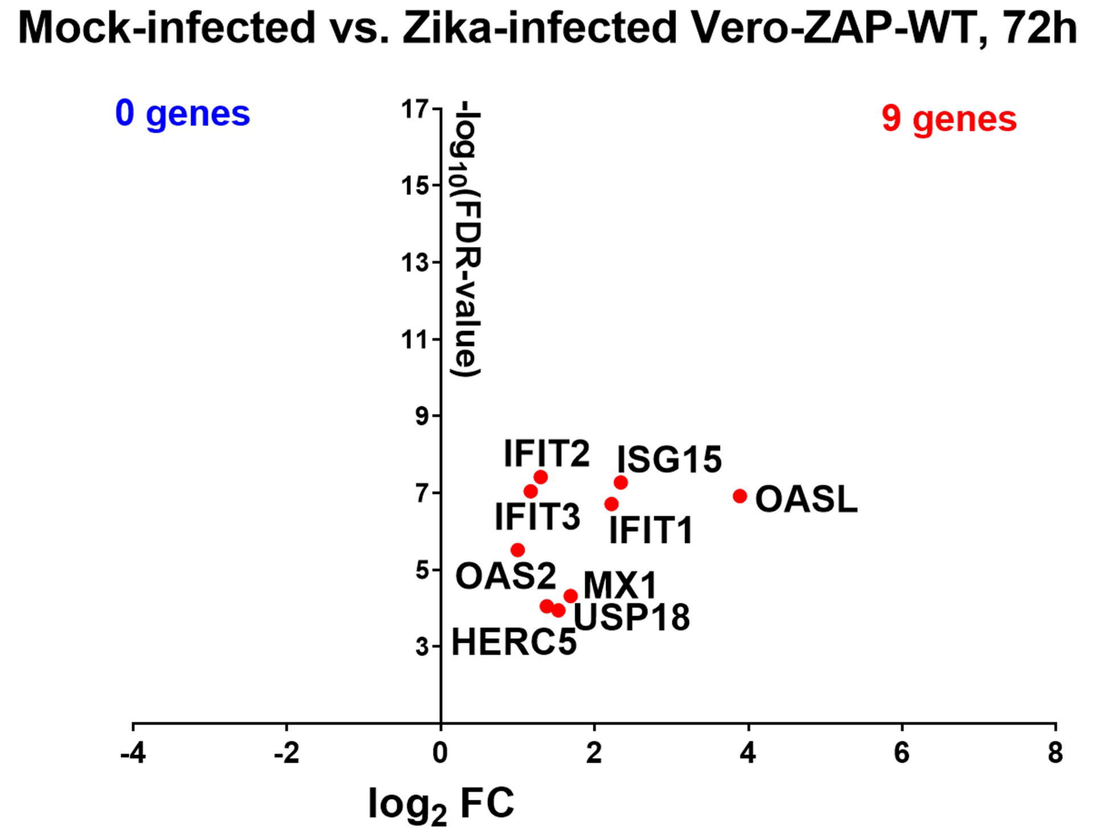
Mock-infected vs. Zika-infected Vero-ZAP-WT, 72h
0 genes
9 genes
IFIT2
ISG15
OASL
IFIT3
IFIT1
OAS2
MX1
USP18
HERC5
-log10(FDR-value)
log2 FC

# D

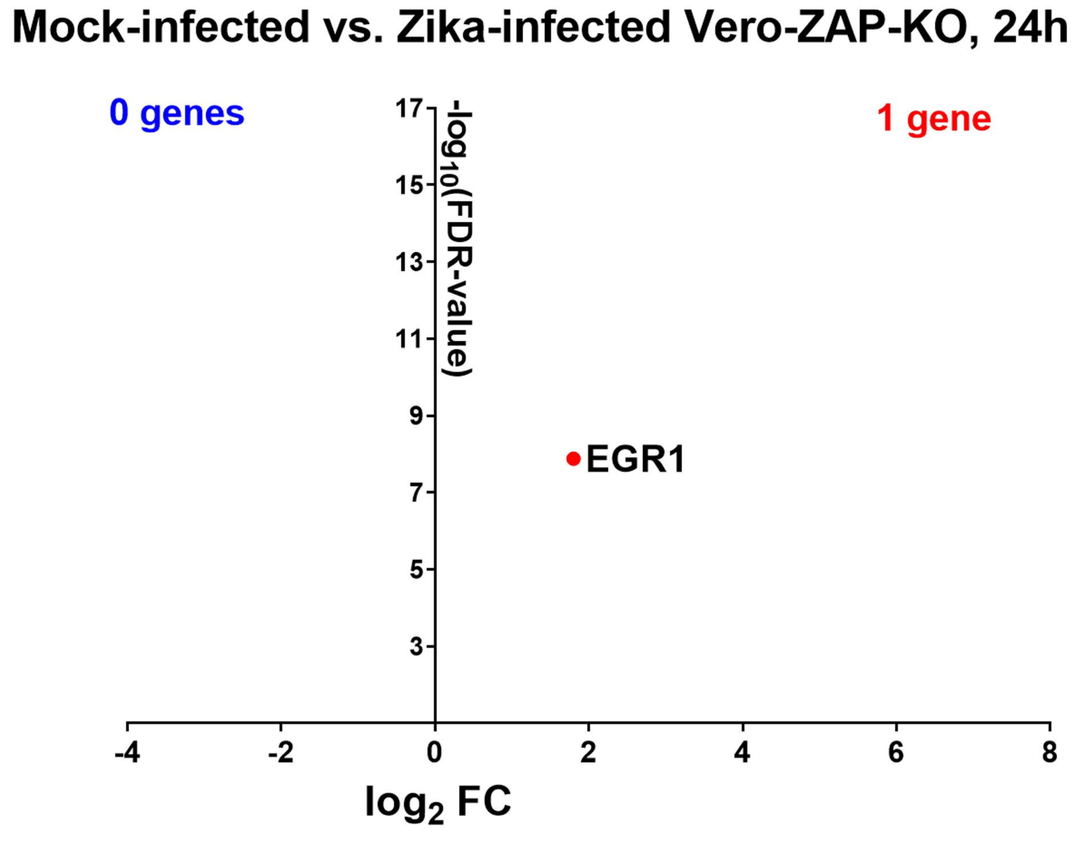
Mock-infected vs. Zika-infected Vero-ZAP-KO, 24h
0 genes
1 gene
EGR1
-log10(FDR-value)
log2 FC

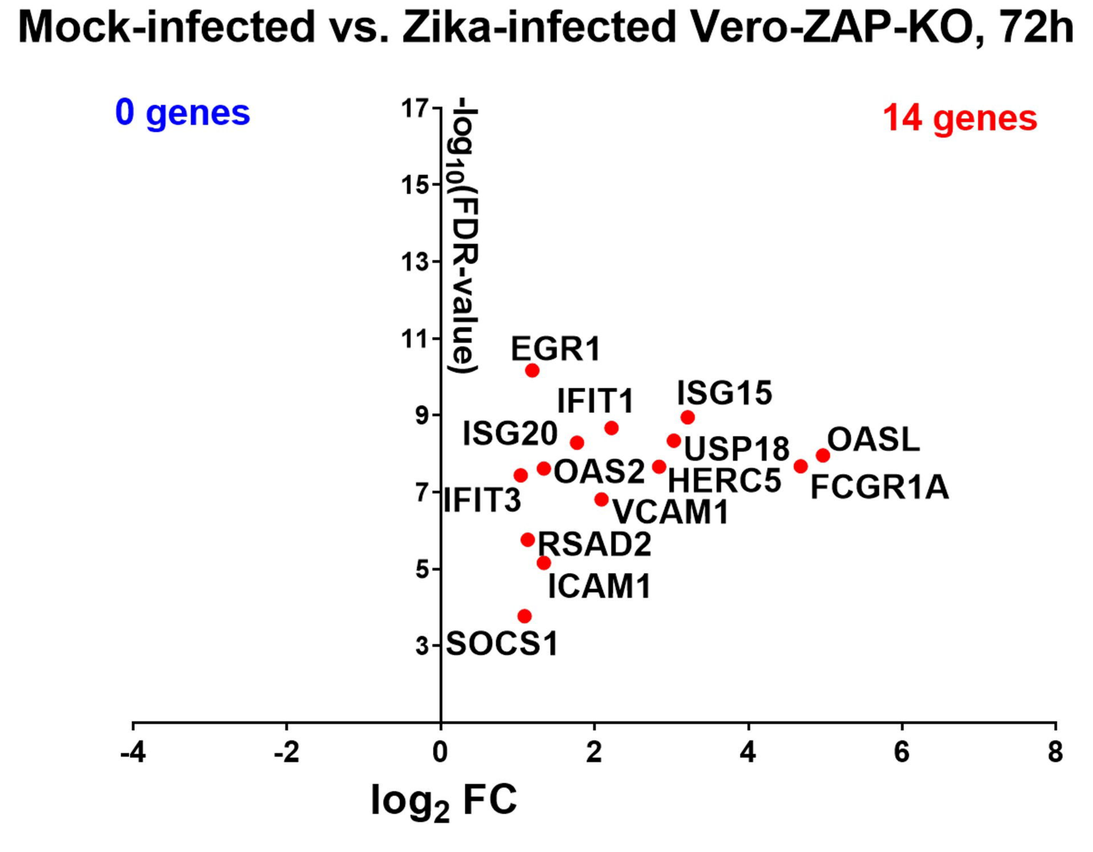
Mock-infected vs. Zika-infected Vero-ZAP-KO, 72h
0 genes
14 genes
EGR1
IFIT1
ISG15
ISG20
USP18
OASL
OAS2
HERC5
FCGR1A
IFIT3
VCAM1
RSAD2
ICAM1
SOCS1
-log10(FDR-value)
log2 FC

A

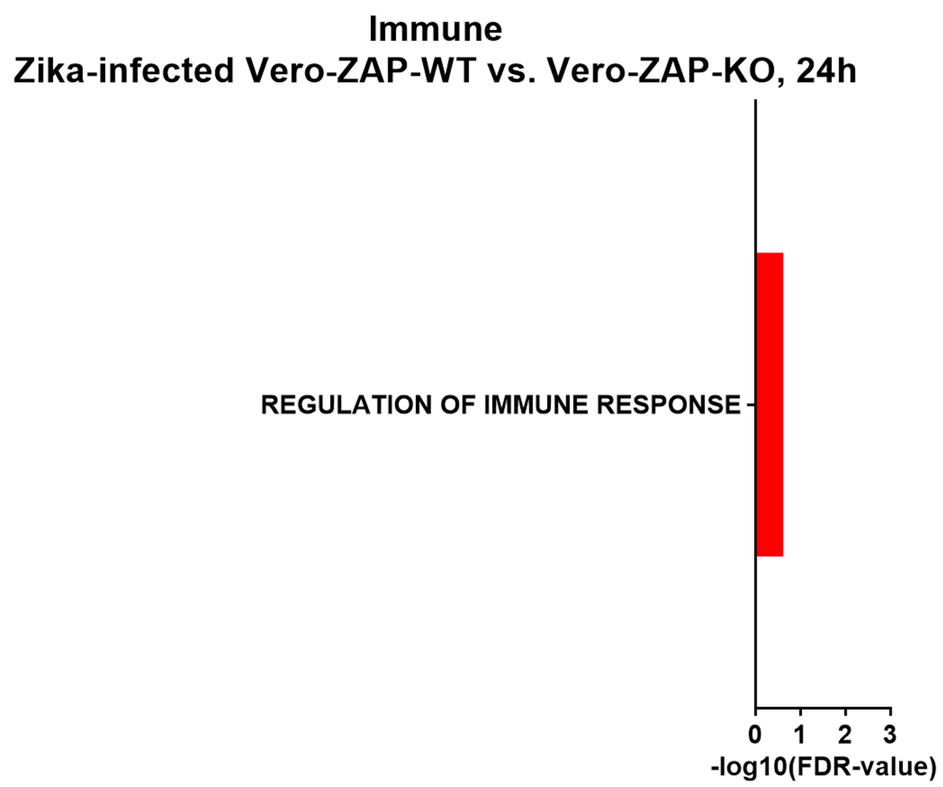
Immune
Zika-infected Vero-ZAP-WT vs. Vero-ZAP-KO, 24h
REGULATION OF IMMUNE RESPONSE
0 1 2 3
-log10(FDR-value)

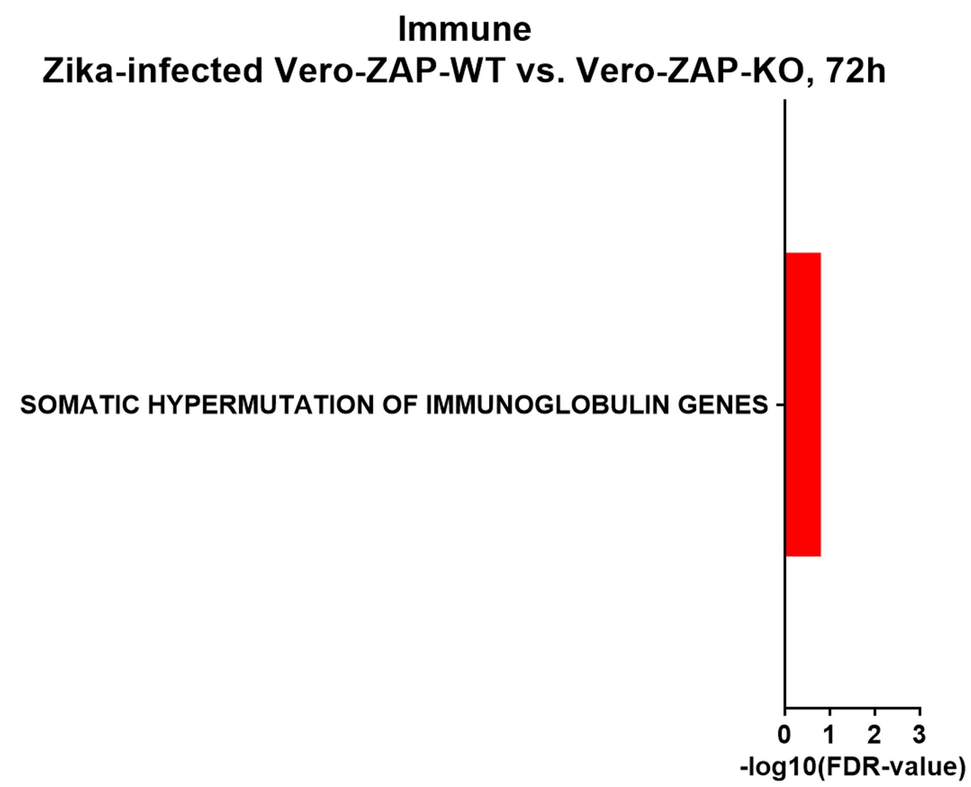
Immune
Zika-infected Vero-ZAP-WT vs. Vero-ZAP-KO, 72h
SOMATIC HYPERMUTATION OF IMMUNOGLOBULIN GENES
0 1 2 3
-log10(FDR-value)

B

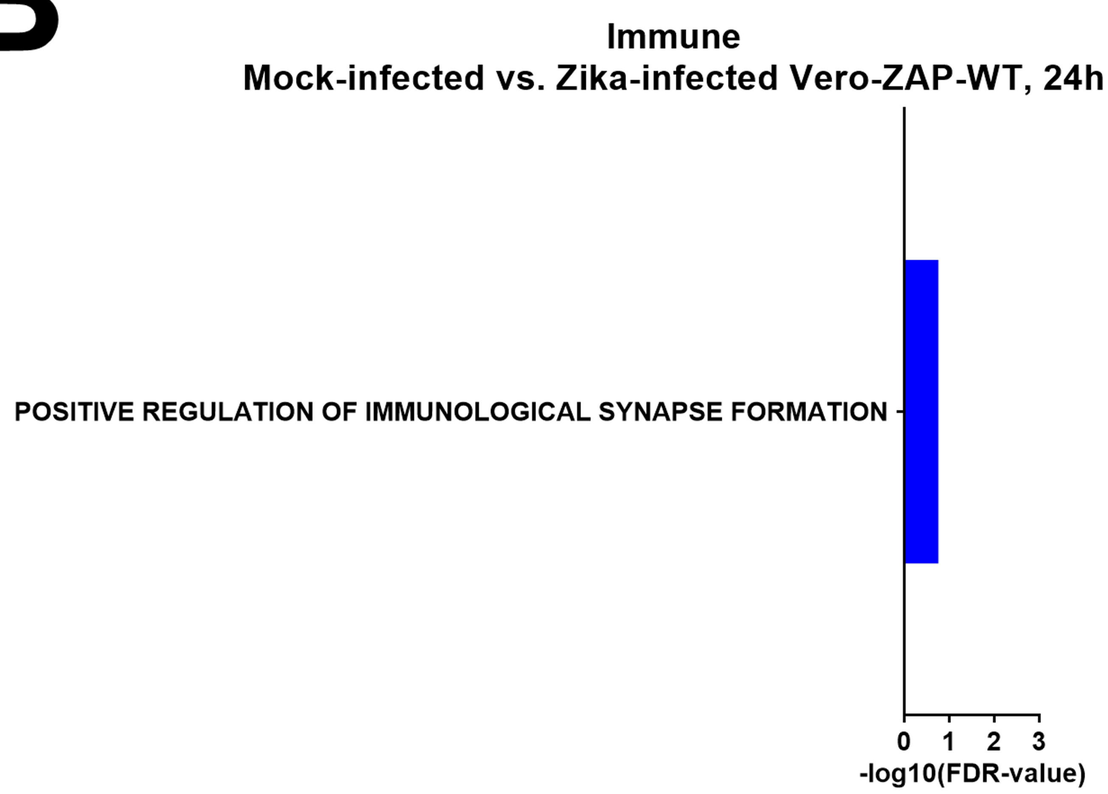
Immune
Mock-infected vs. Zika-infected Vero-ZAP-WT, 24h
POSITIVE REGULATION OF IMMUNOLOGICAL SYNAPSE FORMATION
0 1 2 3
-log10(FDR-value)

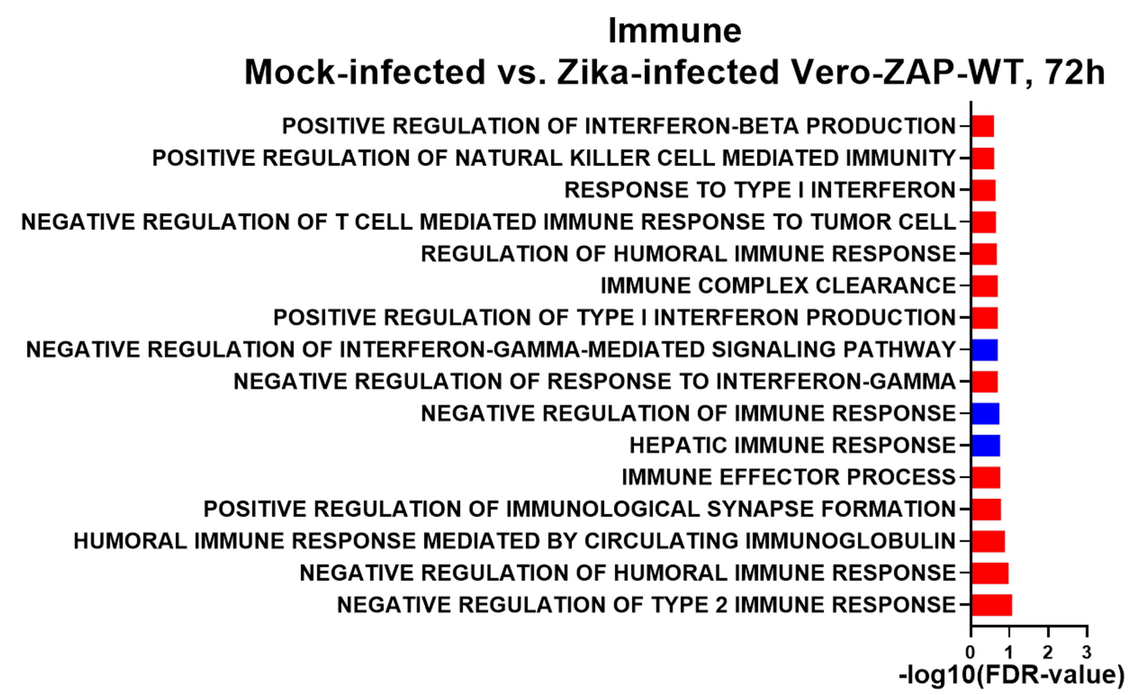
Immune
Mock-infected vs. Zika-infected Vero-ZAP-WT, 72h
POSITIVE REGULATION OF INTERFERON-BETA PRODUCTION
POSITIVE REGULATION OF NATURAL KILLER CELL MEDIATED IMMUNITY
RESPONSE TO TYPE I INTERFERON
NEGATIVE REGULATION OF T CELL MEDIATED IMMUNE RESPONSE TO TUMOR CELL
REGULATION OF HUMORAL IMMUNE RESPONSE
IMMUNE COMPLEX CLEARANCE
POSITIVE REGULATION OF TYPE I INTERFERON PRODUCTION
NEGATIVE REGULATION OF INTERFERON-GAMMA-MEDIATED SIGNALING PATHWAY
NEGATIVE REGULATION OF RESPONSE TO INTERFERON-GAMMA
NEGATIVE REGULATION OF IMMUNE RESPONSE
HEPATIC IMMUNE RESPONSE
IMMUNE EFFECTOR PROCESS
POSITIVE REGULATION OF IMMUNOLOGICAL SYNAPSE FORMATION
HUMORAL IMMUNE RESPONSE MEDIATED BY CIRCULATING IMMUNOGLOBULIN
NEGATIVE REGULATION OF HUMORAL IMMUNE RESPONSE
NEGATIVE REGULATION OF TYPE 2 IMMUNE RESPONSE
0 1 2 3
-log10(FDR-value)

C

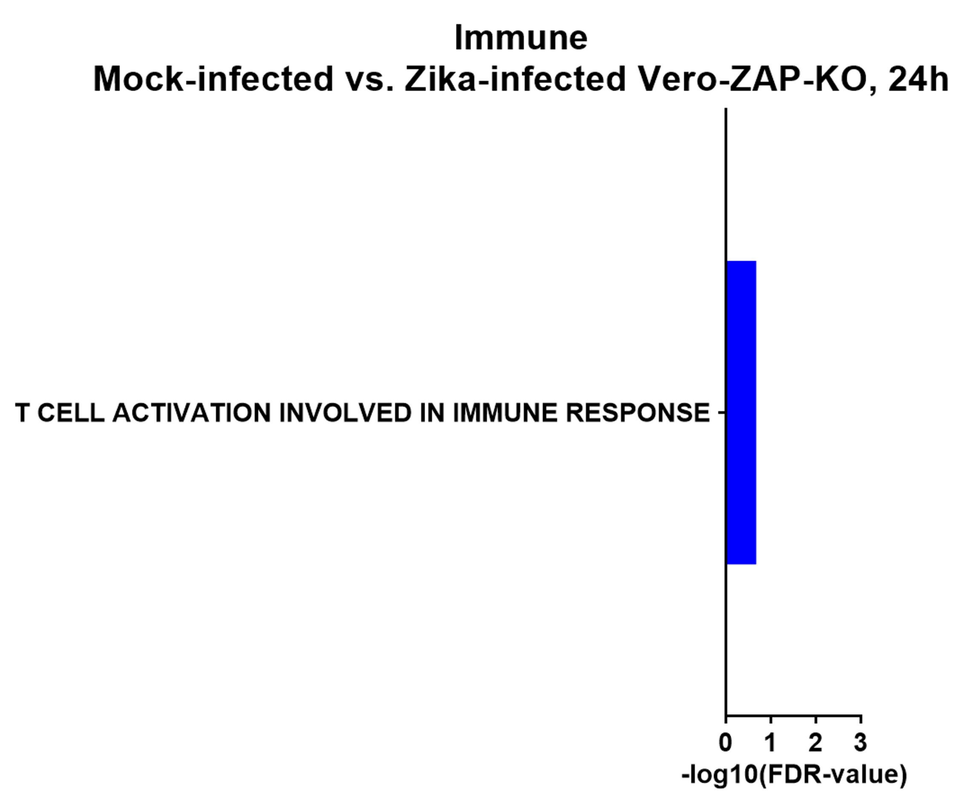
Immune
Mock-infected vs. Zika-infected Vero-ZAP-KO, 24h
T CELL ACTIVATION INVOLVED IN IMMUNE RESPONSE
0 1 2 3
-log10(FDR-value)

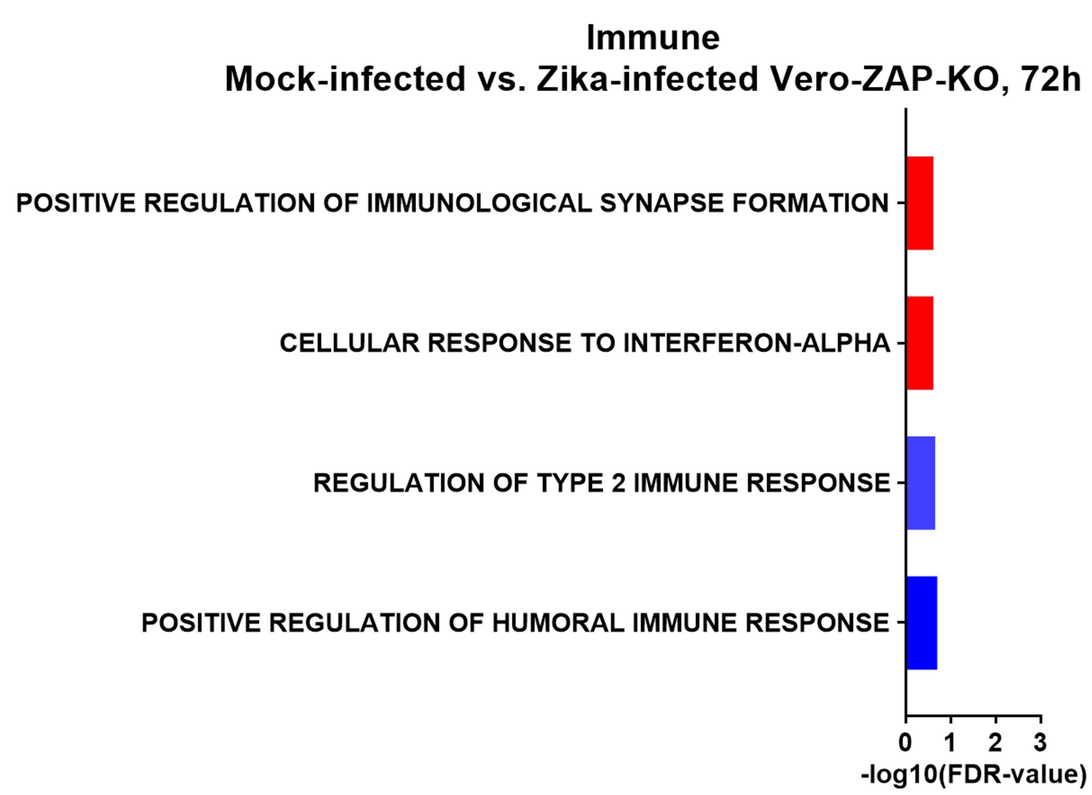
Immune
Mock-infected vs. Zika-infected Vero-ZAP-KO, 72h
POSITIVE REGULATION OF IMMUNOLOGICAL SYNAPSE FORMATION
CELLULAR RESPONSE TO INTERFERON-ALPHA
REGULATION OF TYPE 2 IMMUNE RESPONSE
POSITIVE REGULATION OF HUMORAL IMMUNE RESPONSE
0 1 2 3
-log10(FDR-value)